Increased coral biomineralization due to enhanced symbiotic activity upon volcanic ash exposure

Frank Förster, Stéphanie Reynaud, Lucie Sauzéat, Christine Ferrier-Pagès, Elias Samankassou, Tom E Sheldrake

Increased coral biomineralization due to enhanced symbiotic activity upon volcanic ash exposure

Frank Förster[1]*, Stéphanie Reynaud[2], Lucie Sauzéat[3,4], Christine Ferrier-Pagès[2], Elias Samankassou[5], Tom E. Sheldrake[1]

[1]*Geovolco Team, Department of Earth Sciences, University of Geneva, Genève, Switzerland*

[2]*Ecophysiology Team, Centre Scientifique de Monaco, Monaco, Monaco*

[3]*Laboratoire Magmas et Volcans (LMV), Université Clermont Auvergne, CNRS, IRD, OPGC, F-63000 Clermont-Ferrand, France*

[4]*Institut de Génétique, Reproduction et Développement (iGReD), Université Clermont Auvergne, CNRS, INSERM, F-63000 Clermont-Ferrand, France*

[5]*Sedimentology Group, Department of Earth Sciences, University of Geneva, Genève, Switzerland*

Abstract

Coral reefs, which are among the most productive ecosystems on earth, are in global decline due to rapid climate change. Volcanic activity also results in extreme environmental changes at local to global scales, and may have significant impacts on coral reefs compared to other natural disturbances. During explosive eruptions, large amounts of volcanic ash are generated, significantly disrupting ecosystems close to a volcano, and depositing ash over distal areas (10s - 1000s of km depending on i.a. eruption size and wind direction). Once volcanic ash interacts with seawater, the dissolution of metals leads to a rapid change in the geochemical properties of the seawater column. Here, we report the first known effects of volcanic ash on the physiology and elemental cycling of a symbiotic scleractinian coral under

laboratory conditions. Nubbins of the branching coral *Stylophora pistillata* were reared in aquaria under controlled conditions (insolation, temperature, and pH), while environmental parameters, effective quantum yield, and skeletal growth rate were monitored. Half the aquaria were exposed to volcanic ash every other day for 6 weeks (250 mg L^{-1} $week^{-1}$), which induced significant changes in the fluorescence-derived photochemical parameters (Φ_{PSII}, F_v/F_m, NPQ, rETR), directly enhanced the efficiency of symbiont photosynthesis (P_g, P_n), and lead to increased biomineralization rates. Enhancement of symbiont photosynthesis is induced by the supply of essential metals (Fe and Mn), derived from volcanic ash leaching in ambient seawater or within the organism following ingestion. The beneficial role of volcanic ash as an important micronutrient source is supported by the fact that neither photophysiological stress nor signs of lipid peroxidation were detected. Subaerial volcanism affects micronutrient cycling in the coral ecosystem, but the implication for coral ecophysiology on a reef scale remains to be tested. Nevertheless, exposure to volcanic ash can improve coral health and thus influence resilience to external stressors.

1. Introduction

Tropical coral reefs are one of the most biodiverse and productive ecosystems on the planet, providing essential services to both human and marine life (Van Zanten et al., 2014; Reguero et al., 2018; Souter et al., 2021). However, reef-building corals are susceptible to rapid environmental changes, as observed in recent years and decades due to the detrimental effects of climate change (Hughes et al., 2003; Hoegh-Guldberg and Bruno, 2010). Volcanic eruptions are also known to induce rapid environmental changes from local to global scales, and explosive volcanic eruptions are thought to have significant impacts on reef ecosystems

and coral assemblages compared to other natural disturbances (Houk, 2011). During an explosive volcanic eruption, copious amounts of tephra (fragmented magma in the form of rocks and fine particles) are produced. Depending on the size of the eruption, the amount of released magma can vary from ~10^{11}-10^{15} kg (Self, 2006). A large fraction of the tephra is deposited in the proximity of the volcano, but volcanic ash (tephra diameter < 2 mm), can be dispersed across millions of square km before settling (Ayris and Delmelle, 2012). In the most common small-scale eruptions, the dispersion of tephra fall is usually constrained to several dozen kilometers around the volcano (Sparks et al., 1992), and in the largest eruptions tephra can be distributed over 1000's of kilometers (Kandlbauer et al., 2013). Explosive eruptions on volcanic islands can disrupt marine ecosystems in the vicinity of the volcano (Fig. 1), but can also affect global biogeochemical cycles by enhancing surface ocean availability of micronutrients (Longman et al., 2022).

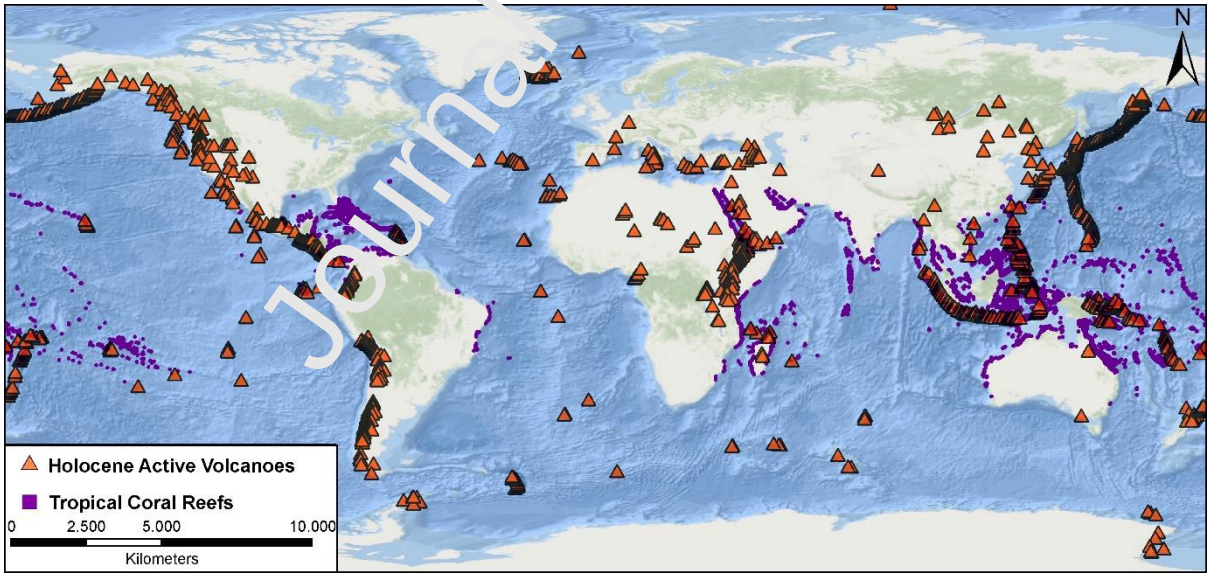

Figure 1: Global distribution map of tropical and subtropical coral reefs and active volcanoes in the Holocene (approx. the last 10,000 years). This map highlights the co-occurrence of tropical reefs and volcanic zones in the last 10,000 years. Data for coral reef distribution was obtained from UNEP-WCMC, WorldFish Centre, WRI, and TNC (2021). Global distribution of warm-water coral reefs,

compiled from multiple sources including the Millennium Coral Reef Mapping Project. Version 4.1. Includes contributions from IMaRS-USF and IRD (2005), IMaRS-USF (2005), and Spalding et al. (2001). Cambridge (UK): UN Environment World Conservation Monitoring Centre. Data DOI: https://doi.org/10.34892/t2wk-5t34 (updated 15.02.23). Volcano Holocene distribution is given in Global Volcanism Program, 2023. [Database] Volcanoes of the World (v. 5.0.4; 17 Apr 2023). Distributed by Smithsonian Institution, compiled by Venzke, E. https://doi.org/10.5479/si.GVP.VOTW5-2022.5.0.

The impact of volcanic eruptions on the aqueous environment depends on the duration and extent of tephra fall, the deposition rate, the remobilization potential and tephra composition. High levels of tephra deposition can result in water turbidity (cloudiness) (Lee, 1996), is linked to a low surface water pH (Dong, 1984; Wall-Palmer et al., 2011), and can directly lead to the smothering of organisms (Eldredge and Kropp, 1985; Ono et al., 2002; Vroom and Zgliczynski, 2011; Wu et al., 2018). Existing studies that investigate the interaction of volcanic ash deposition on coral reefs, all of which are exclusively based on post-eruptive field studies, commonly report mass coral mortality (Heikoop et al., 1996; Vroom and Zgliczynski, 2011; Wu et al. 2018) through smothering, bleaching or coral overgrowth by macroalgae (Schils, 2012). However, if the physical effects of ash fallout do not result in direct smothering, tephra input may have a beneficial role on benthic communities (Frenzel, 1983; Duggen et al., 2007; Pearson et al., 2009), with reefs exhibiting high rates of recovery following exposure to volcanic ash (Smallhorn-West et al., 2020).

When pristine (non-weathered) volcanic ash comes into contact with seawater, metal salt encrustations, that form as a result of the interaction of acidic volcanic gases (e.g. SO_2) with the surfaces of ash particles in the plume, rapidly dissolve (Oskarsson, 1980; Wygel et al.,

2019). This releases acids, minor and trace elements into the surrounding water (Frogner et al., 2001; Ayris and Delmelle, 2012). The potential leaching of volcanic ash depends i.a. (i) on abiotic factors, such as pH and sea surface temperature, governing the complexation, redox state, solubility and bioavailability of metals (Hoffmann et al., 2012), (ii) the geographic deposition of ash, as the ocean locality seems to affect trace metal depletion of ash (Longman et al., 2022) and (iii) leaching partially depends on the amount of metal salts adhering to the surface, which are largely governed by the composition of the source magma (Armienta et al., 2002).

Common leached water-extractable major metal elements are Al, Fe, Mn, Si, Cu, F (> 5 mg/kg ash) (Stewart et al., 2006), and minor elements are As, Ba, Cd, Co, Ni, Pb, Zn (< 5 mg/kg ash) (Ayris and Delmelle, 2012). At high concentrations (above nanomolar concentrations), many of these elements can have a negative impact on coral reefs (Howard and Brown, 1984; Reichelt-Brushett and Harrison, 1999; Sabdono, 2009) by decreasing the growth and reproduction of corals. In addition, since most scleractinian corals live with dinoflagellate algae of the family Symbiodiniaceae (LaJeunesse et al., 2018), which are actively taking up metals (Reichelt-Brushett and McOrist, 2003; Ferrier-Pagès et al., 2018), high metal concentrations can lead to coral bleaching, which is the expulsion of Symbiodiniaceae by the coral host (Meehan and Ostrander, 1997; Peters et al., 1997). However, on the contrary to the above effects, studies have shown that a slight enrichment of certain trace metals (i.e. nanomolar enrichments of Fe, Mn, or Zn) can directly enhance the photosynthesis of the endosymbionts (Ferrier-Pagès et al., 2001, 2005; Biscéré et al., 2018a). As calcification in corals is closely linked to photosynthesis (via the supply of essential molecules for the organic matrix synthesis, calcium carbonate nucleation and change in pH; Tambutté et al., 2011), an enhancement in photosynthesis by metal supply may also lead to an enhancement of

calcification (Biscéré et al., 2018a&b). Some metals, such as Mn, combined with urea, were shown to increase coral calcification (Biscéré et al., 2018b). Also, the slight release of metals through desert dust deposition, or a small supply of metals through zooplankton feeding were proven to be beneficial for corals and their symbionts (Ferrier-Pagès et al., 2018; Blanckaert et al., 2022). There are however limited existing studies that investigate the interaction of volcanic ash deposition on corals, and whether volcanic ash serves as a "nutritional cocktail" or if it is detrimental to the fitness of corals.

This is the first study to investigate the effects of volcanic ash on the photosynthesis and calcification of a symbiotic scleractinian coral maintained under controlled culture conditions. By establishing a connection between coral physiology and volcanic ash fallout, our findings contribute to understanding the impact of tephra deposition on the habitability of volcanic regions for reef-building corals. We further elaborate how subaerial volcanism might affect micronutrient cycling in coral reef ecosystems with the potential to increase coral resistance.

2. Materials and Methods

2.1. Volcanic ash

Pristine (prior to being altered) volcanic ash was gathered on the 9th of April 2021 from a balcony in central Barbados (collector: Dr. John B. Mwansa, location: Airy Hill, Barbados). The ash was collected in plastic trays on the day of the eruption and stored in Zip bags, following the protocol by Witham et al. (2005) and Stewart et al. (2020) to limit the effect of humidity on ash composition. The ash originates from the 2021 Vulcanian eruption of the volcano La Soufrière on St. Vincent, where an 8-15 km high ash plume was generated (Joseph et al., 2022;

Cole et al., 2023). The initial ash input in the atmosphere/stratosphere was high enough to create layers of ash deposits with a thickness between 1-10 mm on the ~175 km eastward located island of Barbados. Barbados is located in the Eastern Caribbean, a group of islands in the Caribbean Sea formed as an expression of a zone, where one lithospheric plate is subducted under another (Macdonald et al., 2000). Actively growing coral reefs are located on the western coast of Barbados (e.g. Lewis, 1960), all of which were subjected to volcanic ash exposure following the 2021 eruption.

The volcanic ash is of andesitic-basaltic composition (Tab. A1) and its main constituents are volcanic silicate glass and the aluminosilicate mineral plagioclase feldspar (Horwell et al., 2023). The particle size distribution (PSD) of the un-sieved ash is unimodal (Fig. A1) and the mean diameter is at 40.6 µm (D_{50}) with a sorting of 3.65 µm, based on descriptive equations by Inman (1952):

$$\sigma_{D=} \frac{D_{84} - D_{16}}{2}$$

$$\sigma = Sorting\ parameter\ (deviation\ measure)$$

$$D_x = x^{th}\ percentile\ of\ the\ cumulative\ PSD$$

2.2. Coral culture conditions

For the experiment, 42 coral fragments ("nubbins", termed after Birkeland, 1976) were cut with a bone clamp from five large parent colonies of the scleractinian coral *Stylophora pistillata* (8-10 nubbins per colony), originating from the Gulf of Aqaba (Red Sea, Jordan). Although not present in the Eastern Caribbean, *S. pistillata* was chosen as it is widespread in many reefs of the world's oceans, is resilient to many stressors, and has been widely used as a model species. Therefore, there is a large amount of data on the effects of different

environmental parameters and stressors, including metals, on this species (eg. Ferrier-Pagès et al., 2003, 2005; Hoogenboom et al., 2012; Metian et al., 2015; Ferrier-Pagès et al., 2018; Biscéré et al., 2018a&b). This allowed us to compare the response obtained with ash-derived metals to the response obtained with other metals, supplied either in the dissolved form (Biscéré et al., 2018a&b), particulate form (Ferrier-Pagès et al., 2018) or as desert dust (Blanckaert et al., 2022). Nubbins (each ~2-4 cm) were attached to a nylon fishing thread, and equally distributed in four tanks (30 L). Coral nubbins were reared under controlled light intensity (200 ± 10 µmol photons m^{-2} s^{-1}), temperature (25° ± 0.2°C), pH (7.93 ± 0.04) and salinity (38.5). The light was provided by 400W metal halide lamps (HPITS, Philips®) on a 12:12 h (light:dark) photoperiod. The tanks were continuously supplied with seawater, pumped at 50 m depth, filtered (20 µm, 5 µm, carbonate buffer), UV treated, and heated using a temperature controller (Elli-Well® PC902 T). Homogenous oxygenation and water circulation in the tank were ensured using a pump (Micro-Jet, MC320, 320L/h; Newa®). After cutting nubbins from the parent colony, the corals remained in this setup over 4 weeks (healing period) while getting fed two times a week with *Artemia salina* nauplii. After healing and one week before the experiment started, the feeding was stopped to avoid the influence of metals supplied through feeding and ash.

2.3. Experimental Setup

Corals were maintained under two different conditions for 6 weeks, with two tanks per condition: a control condition and an experimental condition in which they were exposed to volcanic ash (Fig. 2). The experimental time resembles the median eruption duration of 7 weeks (Siebert et al., 2015), although no two eruptions exhibit the same chronology. Taking two recent examples in the Eastern Caribbean: in the 2021 eruption of La Sourfière (St.

Vincent) the explosive phase lasted 13 days (Cole et al., 2023); and in 1997 two explosive phases at Soufrière Hills Volcano (Montserrat) lasted 8 and 30 days respectively (Druitt et al., 2002).

During the 1997 eruptive periods of Soufrière Hills Volcano the interval between explosions varied between 2.5 and 63 hours (Druitt et al., 2002). In our experimental procedure, three times a week, 2.5 g of unfiltered volcanic ash was mixed with 50 mL of 0.2 µm filtered seawater for 24h within a 50 mL conical test tube, before being added into the experimental tanks (averaging 250 mg L^{-1} $week^{-1}$). This pre-leaching step aimed to increase the subsidence time of ash particles upon introduction to the tanks. The ash enrichment of 250 mg volcanic ash L^{-1} $week^{-1}$ was chosen to have a limited effect on shading and no polyp smothering, as this study aims to develop an understanding of the principles of dilute volcanic ash exposure to corals. Every morning, the seawater inlet was turned off in the tanks and three times a week the volcanic ash suspension was added to the experimental tanks. Water was pumped within each aquarium to ensure uniform temperature, but did not induce turbulence that led to the resuspension of volcanic ash. After 8h/d of ash exposure, the water supply was turned on again, allowing a complete water renewal overnight. Once a week, the tanks were cleaned from ash deposits and algae. This is a crucial step to prevent the overgrowth of corals by fleshy algae, which would affect the growth rate determination. During the experiment, turbidity, pH change, and coral survival were monitored. To guarantee a stable light intensity and to quantify occurring turbidity, daily measurements were conducted using a ULM-500 Light Meter & Logger (Walz GmbH®, Effeltrich, Germany) connected to a quantum sensor (LI-193).

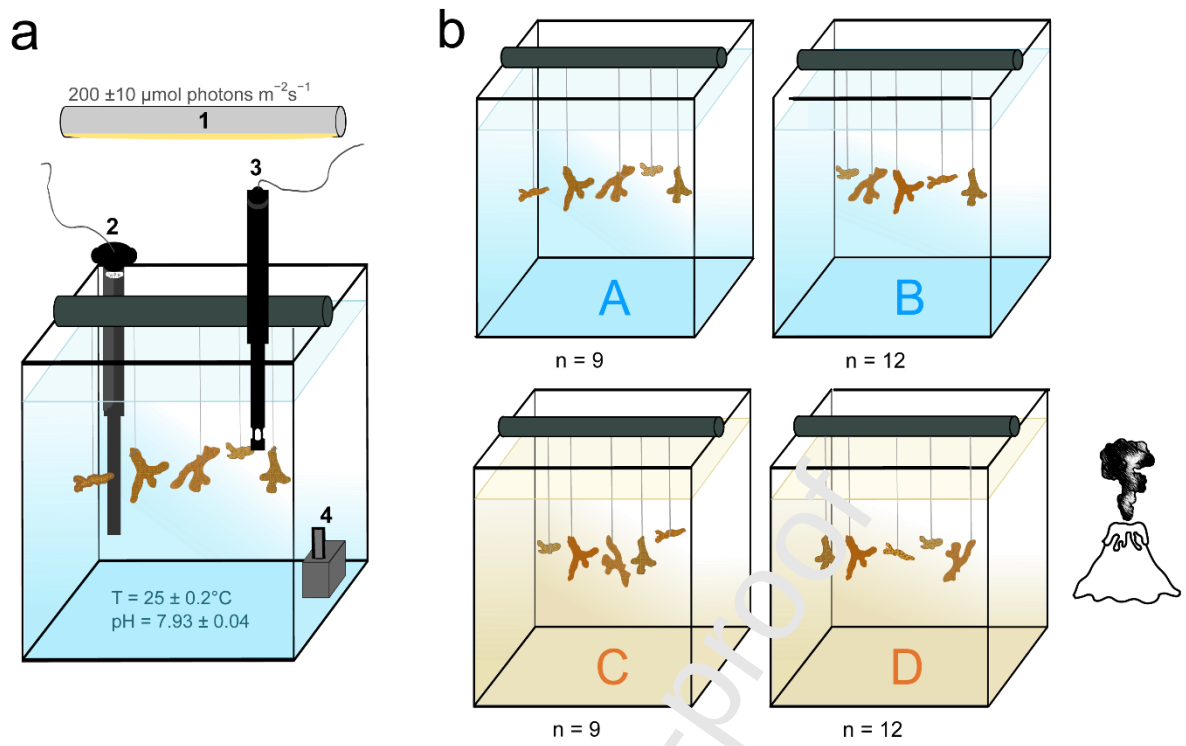

Figure 2: Experimental setup. (a) Model tank setup with highlighted equipment (1 = light source, 2 = heating element, 3 = pH, conductivity, and temperature probe, 4 = water pump). Not visible in this graphic is the seawater inlet and outlet. Light intensity and temperature were kept constant at 200 ± 10 µmol photons m^{-2} s^{-1} and 25 ± 0.2 °C, respectively. (b) Schematic experimental design. The setup includes four tanks in total, two of which were kept at control condition (A and B), while the other two were supplied with 2.5 g volcanic ash three times a week for 6 weeks (averaging 250 mg volcanic ash L^{-1} $week^{-1}$) (C and D). *n* indicates the number of nubbins of *Stylophora pistillata* added to each tank. After the experimental runtime, nubbins were frozen for further measurements.

2.4. Physiological measurements

2.4.1. Photosynthesis and respiration rate

At the end of the experiment, rates of net photosynthesis (P_n), gross photosynthesis (P_g), and respiration (R) were estimated from the increase (for P_n and P_g) or decrease (for R) in the O_2 concentration in seawater, where P_g is the sum of the absolute values of P_n and R. Coral

fragments (n = 6 per condition, 3 per tank) were individually put in Plexiglass® chambers (60 ml) filled with 0.45-µm-filtered seawater. The incubation medium was kept at 25°C and constantly agitated using a magnetic stirrer. The oxygen concentration was measured with an oxygen sensor (polymer optical fiber, PreSens®) connected to an Oxy-4 (channel fiber-optic oxygen meter, PreSens®) and was recorded with the Oxy4v2-30fb software. P_n was measured at 200 µmol photons m^{-2} s^{-1} irradiance for 45 min while R was measured in the dark. The calibration was done before the experiment on 100% O_2-saturated and N_2-saturated (0% O_2) seawater. Data was normalized to the coral surface area and the total amount of symbionts and is given as µmol O_2 h^{-1} cm^{-2}, or pmol O_2 symbiont $cell^{-1}$, respectively. After the measurement, the nubbins were frozen (-20°C) for further analysis of the symbiont density, total protein content, and chlorophyll *a* and c_2 content. The skeletal surface area was then determined using the single dip wax technique (Stimson and Kinzie, 1991).

2.4.2. Symbiont density, protein holobiont content, and chlorophyll *a* and c_2 content

Tissue and symbiont were separated from the skeleton using a Water-pick and 0.22 µm-filtered seawater. Connected tissue layers were sequentially ground in a potter (Wheaton®). The solution was then distributed into 3 sub-samples for the following measurements.

A 100 µl sub-sample was diluted in 9.9 ml of Isoton II (Beckman Coulter®, Ic, 8546719) and used to assess the number of endosymbionts with a Z1 Coulter Particle Counter (Beckman Coulter®). Measurements were made in triplicates for each sample and only particles with a size greater than 7 µm were counted.

Another 500 µl subsample was used to determine the protein concentration of each sample, using the Bradford Assay (Thermo Scientific™ Protein Dosage Pierce™ Coomassie kit reference: 23200) according to Smith et al. (1985). Each sub-sample was mixed with 0.5 M

NaOH and added in triplicate to a 96-well microplate, together with a calibration curve. The calibration curve was made with 2 mg/mL BSA (Bovine Serum Albumin) and multiple dilution steps (0, 50, 100, 200, 500, 1000, 1500, and 2000 µg/mL). The Pierce Coomassie Assay Reagent was then added to all wells, and solutions were homogenized with a microplate vortex. After the incubation of the microplate for 30 min at 60°C, the absorbances were read on a spectrophotometer (Xenius®; SAFAS) at a wavelength of 595 nm. The protein content was normalized to the skeletal surface area.

The last 5 mL sub-sample was centrifuged at 8000 G for 10 min at 4 °C. The supernatant was discarded and the concentrate containing symbionts was resuspended in filtered seawater. The operation was repeated three times before 3 ml Acetone (99%) was added to the symbiont concentrate. The final solution was covered in aluminum foil and stored for 24h at 4 °C. After centrifugation at 11000 G for 15 min at 4°C, 300 µL of the supernatant was added in triplicate in a quartz microplate. Chlorophyll *a* and c_2 concentrations were determined using a spectrophotometer (Xenius®; SAFAS) at the absorbances of 663 and 616 nm. Concentrations were calculated following the equations by Jeffrey and Humphrey (1975) and Ritchie (2006) and normalized to the skeletal surface area and total symbiont amount.

2.4.3. Chlorophyll fluorescence measurements

Chl *a* fluorescence of photosystem II (PSII) was measured at the same time of the day, during the whole experiment using a PAM fluorometer (DIVING-PAM, Walz®, Germany) and on 6 nubbins per condition. The minimal (F_0) and maximal (F'_m) fluorescence yields at 200 µmoles photons m^{-2} s^{-1} were measured by applying a weak pulsed red light (max. intensity <1000·µmol photons $m^{-2}·s^{-1}$, width 3 ms, frequency 0.6 kHz), and a saturating pulse of actinic light (max. intensity > 8000·mmol·photon·$m^{-2}·s^{-1}$, width 800·ms), respectively. The effective

quantum yield of photosystem II (Φ_{PSII}), which reflects the coral photophysiological state and indicates the amount of energy used in photochemistry (Ralph and Gademann, 2005), was then calculated according to Genty et al. (1989) and Franklin and Badger (2001) as

$$\Phi_{PSII} = \frac{F'_m - F_0}{F'_m}$$

The maximum photosynthetic efficiency in dark-adapted corals ($F_v/F_m = (F_m - F_0)/F_m$, where F_v is the variable fluorescence) and the relative electron transport rate (rETR = Φ_{PSII} *x 0.5 x* PAR (photosynthetic active radiation)) were used to assess the efficiency of the PSII between treatments according to Ralph and Gademann (2005). Rapid light curves (RLC) were obtained from dark-adapted nubbins (10-15 min) at the end of the experiment by illuminating corals for 10s periods, eleven times from 0 to 1956 µmol photons m^{-2} s^{-1} (0, 10, 17, 26, 41, 74, 130, 220, 664, 1032, 1956 µmol photons m^{-2} s^{-1}).

During measurements, the fiber was maintained perpendicular to the coral's surface using a fixed distance of 5 mm. Values of light intensities received by the corals during RLCs were obtained using the internal Light-Calibration program of the Diving-PAM. The amount of energy dissipated as heat (NPQ) is defined by Bilger and Björkman (1990) as

$$\mathrm{NPQ} = \frac{F_m}{F'_m} - 1$$

After the RLC treatment, coral nubbins remained in darkness to assess the NPQ recovery after 1, 3, and 10 min.

The recorded F_v/F_m, Φ_{PSII}, rETR, and NPQ were plotted as a function of PAR. The data is visualized by using the WinControl_v.3.29 program (Walz GmbH®, Effeltrich, Germany).

2.4.4. Lipid peroxidation

Lipid peroxidation levels were assessed *via* the thiobarbituric acid reactive substances (TBARS) assay, according to Oakes and Van Der Kraak (2003). Malondialdehyde (MDA) is formed as a major lipid peroxidation product and its reaction with thiobarbituric acid is one way to quantify oxidative stress. Snap-frozen coral fragments (n = 6 per condition) were placed in Eppendorf vials filled with 200 µl buffer (KCl (1.15%) solution with 35 µM butylhydroxytoluene (BHT)) and homogenized in ice using an ultrasonic rod (70 kHZ, Vibra-Cell™; Bioblock Scientific). Samples were centrifuged at 10000 G for 10 min at 4 °C, and an aliquot of the supernatant was used for protein determination using the Bradford protein assay (Bradford, 1976) and standardized to 0.8 µg µl^{-1}. A standard curve was made with tetramethoxypropane hydrolyzed into MDA. Sample and standard range solutions were then transferred to pyrogen Eppendorf and incubated for 30 min at 95 °C with acetic acid (20%), TBA (0.8 %), Milli-Q water, and sodium dodecyl sulfate (8.1%) solution. After cooling for 10 min at room temperature in the dark, 100 µl de-ionized water and 500 µl n-butanol were added and slowly vortexed to mix the two phases. Samples were centrifuged at 10000 G for 10 min at 15 °C. 150 µl of the supernatant (organic phase) of each sample was added in duplicate to a 96-well black plate. The fluorescence is read every minute for 3 minutes at 515 nm and 553 nm on a spectrophotometer (Xenius®; SAFAS). Results were normalized to the protein content and expressed as nmol MDA per mg protein^{-1}.

2.4.5. Skeletal growth rate

The skeletal growth of each coral fragment (n = 42) was monitored by its gain in weight over the experimental runtime. Measurements were performed once per week according to the buoyant weight technique (Jokiel et al., 1978), using a Mettler Toledo XP205 balance

(accuracy ± 0.01 mg). The calcification rate was calculated *via* the equation given in Reynaud et al. (2002):

$$G = \sqrt[n]{\frac{Pn}{P_0} - 1}$$

with G as calcification rate (% days^{-1}), n the time (days), P_n the weight (g) after n days of culture, and P_0 the initial weight (g).

2.5. Major and trace element analysis

Major and trace element compositions were quantified on volcanic ash, coral host (tissue) and symbionts using an ICP-OES (Agilent 5800) and a QQQ-ICP-MS (Agilent 8900) respectively at the Laboratoire Magmas et Volcans (LMV). Before measurements, tissue and symbionts were separated from the skeleton using a Water-pick with de-ionized water. After the mixture was sequentially ground in a potter (Wheaton®), the sample was centrifuged at 8000 G for 10 min at 4 °C. The supernatant containing coral tissue was transferred to a seperate 50 mL conical tube and the concentrate containing symbionts was resuspended in deionized water. The operation was repeated three times. Before metal analyses, symbionts and host tissue were freeze-dried. At the exception of ash samples dedicated to major element quantification which were melted with lithium metaborate and then dissolved with nitric acid (0.5N), all the samples were first dissolved in 15 concentrated HNO_3-H_2O_2 (for coral host and symbionts) or HF-HNO_3-HCl (for ash) mixture in Savillex® beakers at 100°C for at least 48h. To ensure complete digestion, this step was repeated three times. Once fully digested, solutions were evaporated at 80°C to avoid losses by evaporation of highly volatile elements like selenium (Se), and then diluted in low concentrated nitric solution (0.5N HNO_3). The concentrations were then calculated using calibrations curves performed with a blank and different dilutions

of multi-element standard solutions. For trace elements, indium (In) was used as internal standard to assess analytical drift. The accuracy and precision of both major and trace element concentrations are based on complete duplicate and re-run analyses of samples as well as the simultaneous analysis of matrix-matched certified reference materials (1577c, BHVO-1, BHVO-2, DR-N). Our measured values are within the uncertainty of previously published results and reproducibility is, on average, better than 5% (2σ). Major and trace element concentrations in volcanic ash are reported in wt.% and ppm (μg g^{-1}) (Tab. A1). Element concentrations in coral host and symbionts are reported and presented as mass normalized per skeletal surface area (ng cm^{-2}) and can be found also in ppm (μg g^{-1}) dry weight in Tab. A2. Note that all chemical analyses were carried out in laminar flow hoods using double-distilled acids to avoid exogeneous contaminations.

2.6. Statistical Analysis

Data were examined for normal distribution with the Shapiro-Wilk test and were checked for homoskedasticity with the Levene test. For normally distributed data, a single one-way ANOVA was performed. If the normality test was rejected, the non-parametric Wilcoxon-Mann-Whitney test (WMW) was performed. If the homoskedasticity test was rejected, but the data is verified to be normally distributed, the Welch t-test (Welch) was performed. Differences between groups were termed statistically significant when $p \leq 0.05$ in all cases. Levels of significance are indicated as p-value > 0.05 (not significant), p-value ≤ 0.05 (*), p-value ≤ 0.01 (**), and p-value ≤ 0.001 (***). Statistical analysis was performed with R 4.2.0.

3. Results

The statistical tests (ANOVA, WMW, and Welch) are listed in the supplementary material: Table A3 for the physiological parameters and photosynthesis and respiration rates, and Table A4 for the effective quantum yield (Φ_{PSII}). Tables A5, A6, and A7 for the results of RLC measurements (rETR, F_v/F_m, and NPQ, respectively) and Table A8 for the weekly skeletal growth rate.

3.1. Abiotic environmental parameters

Immediately after the addition of the ash to the aquaria, turbidity decreased PAR by 16 ± 9 %, and also minorly affected the irradiance on the neighboring control tanks (Fig. A2a). Suspended ash particles subsequently sedimented, so that the initial light intensity of 200 ± 10 µmol photons m^{-2} s^{-1} was restored 2-4 hours after the ash addition (Fig. A2a). Furthermore, the addition of volcanic ash into the tanks did not change the monitored pH (Fig. A2b).

3.2. Physiological measurements

The constant ash supply did not affect the symbiont density (ANOVA, p = 0.08; Fig. 3a) nor the total protein content (Welch, p = 0.2; Fig. 3b). Noticeably, the measured values in the ash-exposed nubbins exhibited high precision (Symbiont density 4.92% RSD; Protein content 9.66% RSD), while the control nubbins showed larger variation in the number of symbionts and total protein content per surface area (30.61% RSD and 41.39% RSD, respectively). A similar trend to the symbiont density can be observed in the total chlorophyll *a* and c_2 content per surface area, although in this case a statistically significant increase in the ash-exposed nubbins was detected (ANOVA, $p < 0.05$; Fig. 3c). Normalized per symbiont cell, there was no statistical difference in the chlorophyll *a* and c_2 content (WMW, p = 0.3; Fig. 3d). Also, in the 6 weeks of ash exposure, no difference in lipid peroxidation could be measured (ANOVA, p = 0.7; Fig. A3).

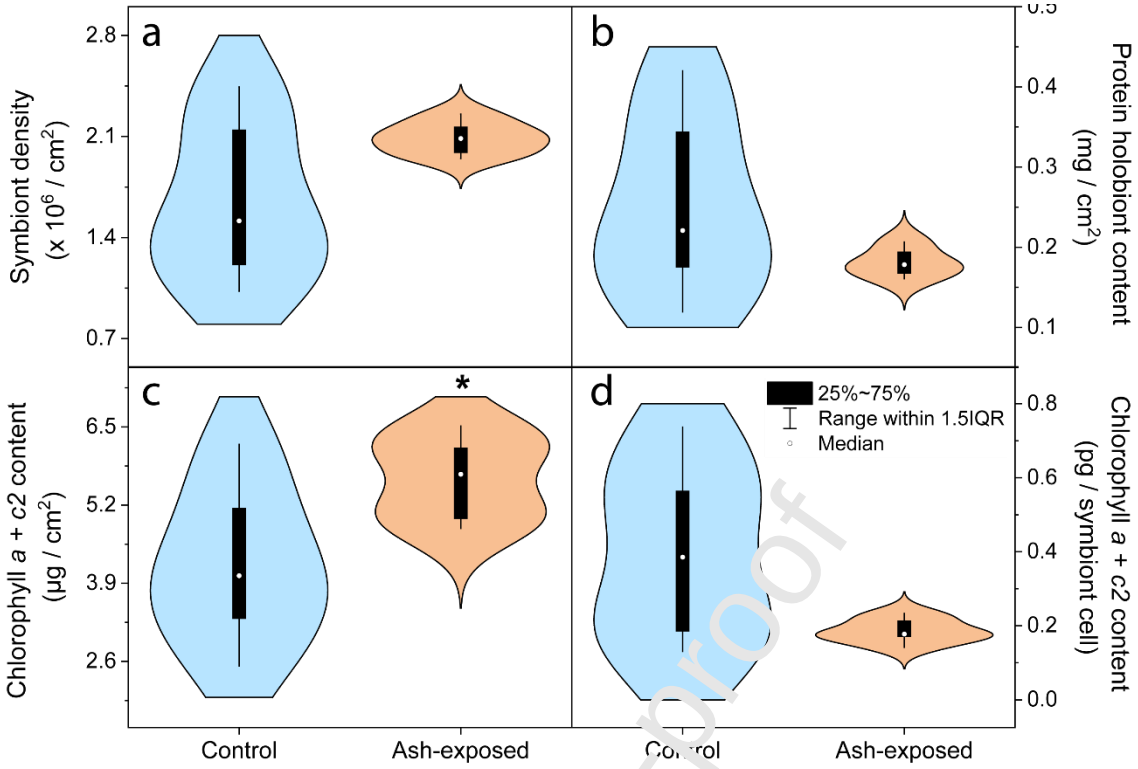

Figure 3: Physiology of *Stylophora pistillata* reared in the control condition (blue) and after 6 weeks of exposure to 250 mg volcanic ash L^{-1} $week^{-1}$ (orange) (n = 6 per condition). Violin plots represent the (a) Symbiodiniaceae density as number of endosymbionts per skeletal surface area, (b) total protein holobiont content normalized per skeletal surface area, (c & d) total chlorophyll *a* + c_2 content normalized per skeletal surface area and per symbiont cell, respectively. The white point represents the median value, the black box delimits the 1st and 3rd quartile and the whiskers give the range within 1.5 of the Inter-Quartile Range (IQR, defined as Q3-Q1). The width of the violin plots indicates data density. Statistically significant differences between treatments are represented by asterisks (*), with an indication of the level of significance in the number of asterisks.

3.2.1. Photosynthesis and respiration rate

The constant ash supply over 6 weeks led to a measurable increase in the photosynthesis rate of the nubbins normalized to surface area and symbiont cell (ANOVA, $p < 0.0001$ and $p < 0.004$, respectively; Fig. 4a & b). On average, the net oxygen production rate (P_n) per surface area and symbiont cell of the ash-exposed Symbiodiniaceae was respectively 255 % and 191

% higher than the ones grown as control. The respiration rate (R) per surface area between ash-exposed and control nubbins did not show a difference (ANOVA, $p = 0.1$; Fig. 4a), while the normalization per symbiont cell displayed higher oxygen consumption in the control nubbins (Welch, $p < 0.02$, Fig. 4b). The gross oxygen flux (P_g) (sum of net oxygen production and consumption) per surface area showed a statistically significant increase in the ash-conditioned nubbins (ANOVA, $p < 0.02$; Fig. 4c), while no difference was observed in the P_g per symbiont cell (W, $p = 0.75$, Fig. 4d).

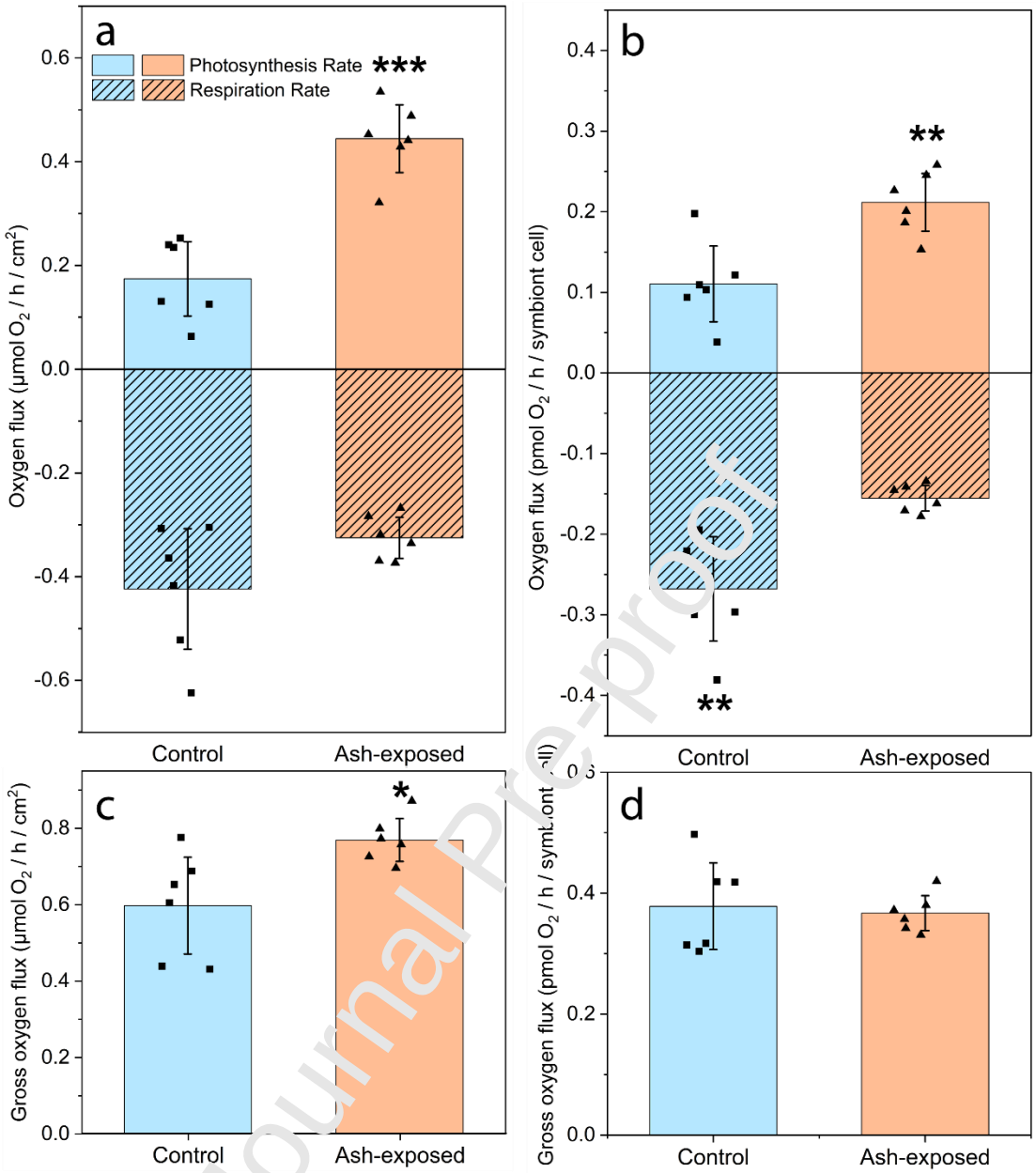

Figure 4: Photosynthesis- and respiration rates in *Stylophora pistillata* reared in the control condition (blue) and after 6 weeks of exposure to 250 mg volcanic ash L^{-1} $week^{-1}$ (orange) (n = 6 per condition). Bar plots represent the (a & b) oxygen flux (oxygen production = photosynthesis, oxygen consumption = respiration) normalized per skeletal surface area and per symbiont cell, respectively. (c & d) Gross oxygen flux (sum of respiration and photosynthesis rate) normalized per skeletal surface area and per symbiont cell, respectively. The height of individual bars represents the mean of the displayed data ± SD. Statistically significant differences between treatments are represented by asterisks (*), with an indication of the level of significance in the number of asterisks.

3.2.2. Photophysiology

Chlorophyll fluorescence measurements revealed while nubbins in both conditions showed a similar effective quantum yield of PSII before the experiment (0.3; Fig. 5), after 4 days the exposure to volcanic ash led to a consistently higher Φ_{PSII} than the nubbins in the control condition (ANOVA, $p < 0.005$; Tab. A4). The addition of ash led to a steady increase of Φ_{PSII} over the entire experiment, whereas the control nubbins exhibited constant Φ_{PSII} – values around 0.3. After 6 weeks, ash-exposed nubbins displayed a Φ_{PSII} – value 231% higher than those of the control nubbins.

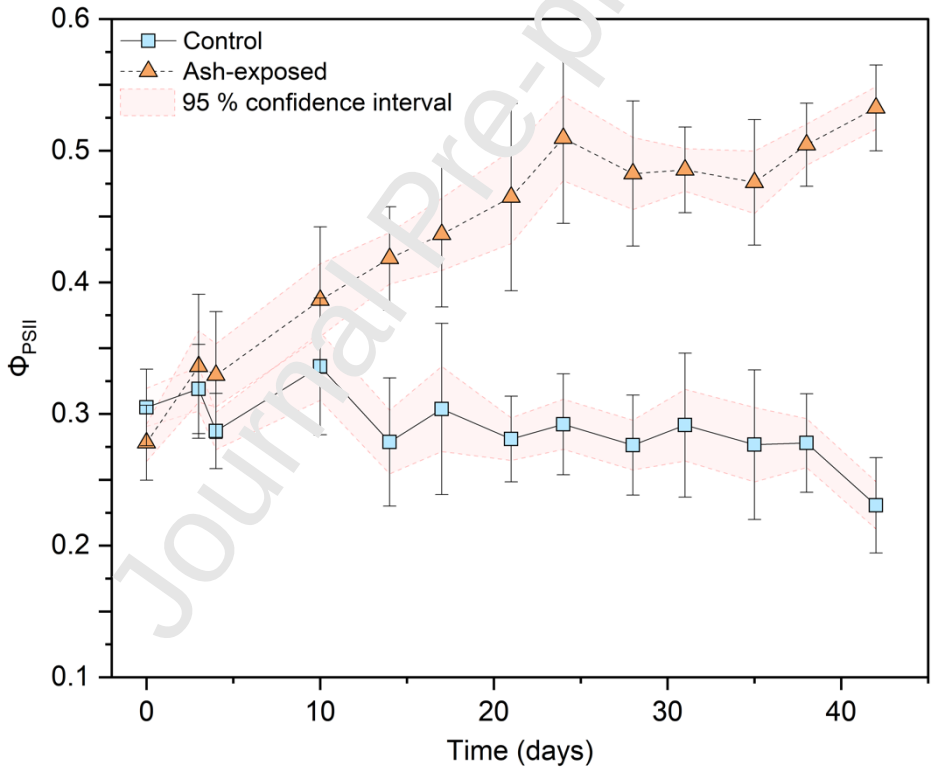

Figure 5: Effective quantum yield of PSII (Φ_{PSII}) of *Stylophora pistillata* reared in the control condition (blue) and during 6 weeks of exposure to 250 mg volcanic ash L^{-1} $week^{-1}$ (orange) (n = 6 per condition). Data is presented as mean ± SD with a 95% confidence interval.

The RLC curves showed that at low irradiance (0 – 220 µmol photons m^{-2} s^{-1}) the F_v/F_m values for the ash-exposed nubbins were significantly higher than for the control nubbins (Fig. 6b). Dark-adapted ash-exposed nubbins exhibited a F_v/F_m 213% higher (0.597) than the nubbins grown in the control condition (0.280) at PAR = 0. At higher light intensity (> 664 µmol photons m^{-2} s^{-1}) no difference between conditions could be observed.

The relative electron transport rate (rETR) for PSII increased in both conditions with increasing light intensity (Fig. 6c). The rETR of ash-exposed corals was elevated at lower irradiances (0 – 220 µmol photons m^{-2} s^{-1}) compared to control nubbins. At higher PAR (> 664 µmol photons m^{-2} s^{-1}) the rETR values of nubbins in both conditions were within the error range (at PAR = 664, WMW, $p = 0.9$; Fig 6c) with statistically significantly higher values for control nubbins at 1032 and 1956 µmol photons m^{-2} s^{-1} (ANOVA, $p < 0.04$ and $p < 0.01$, respectively).

Non-photochemical quenching (NPQ) in ash-exposed and control nubbins increased with increasing light intensity. At the lowest irradiance (0 and 10 µmol photons m^{-2} s^{-1}) similar amounts of heat were dissipated. At PAR > 17 µmol photons m^{-2} s^{-1}, the NPQ levels for the control condition were systematically higher than in the ash-supplied condition, with the difference in NPQ increasing with higher irradiance (for PAR = 1956; ANOVA, $p < 0.00002$; Fig. 6d). Nubbins exposed to ash also exhibited smaller variances in the calculated NPQ for higher light intensities. After 1 min recovery, the NPQ relaxed to a proportion of 6% for control nubbins. Conversely, for ash-exposed nubbins an increase in NPQ was observed after the RLC treatment, increasing to 1.15 in the minute following the last saturating pulse (Fig. A4). After 10 min, the NPQ for control and ash-exposed nubbins recovered 50% and 28%, respectively.

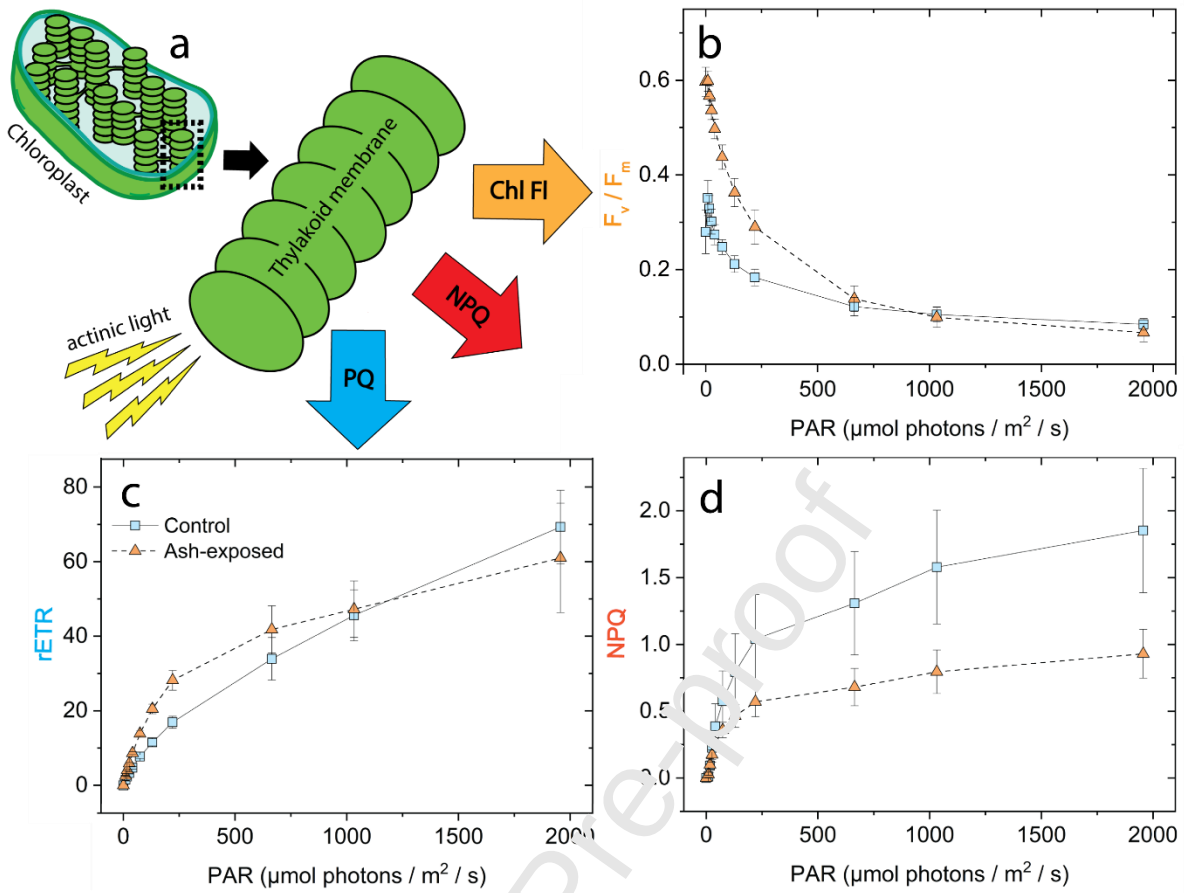

Figure 6: Light-response of *Stylophora pistillata* reared in the control condition (blue) and after 6 weeks of exposure to 250 mg volcanic ash L^{-1} $week^{-1}$ (orange) (n = 6 per condition) to rapid light curves (RLC). (a) Simplified schematic depiction of calculable deexcitation pathways (PQ = photochemical quenching, Photosynthesis; NPQ = non-photochemical quenching, heat dissipation; Chl Fl = Chlorophyll Fluorescence) after an actinic light pulse stimulates photochemical reactions in the thylakoid membrane in the Symbiodiniaceae. (b) The maximum quantum yield of PSII (F_v/F_m), (c) relative electron transport rate (rETR), and (d) NPQ of dark-adapted nubbins. Data is presented as mean ± SD.

3.2.3. Skeletal growth rate

Over the entire experiment, coral nubbins frequently exposed to volcanic ash experienced faster growth. At the end of the 6 weeks, a higher mean daily calcification rate (ANOVA, $p < 0.002$; Fig. 7a) was measured. With increasing duration of the experiment, the systematic

difference in growth rate between the two conditions became clearer (after 6 weeks; ANOVA, $p < 0.0002$; Tab. A8). After 6 weeks the ash-exposed nubbins grew on average twice as much as the control nubbins (Fig. 7b).

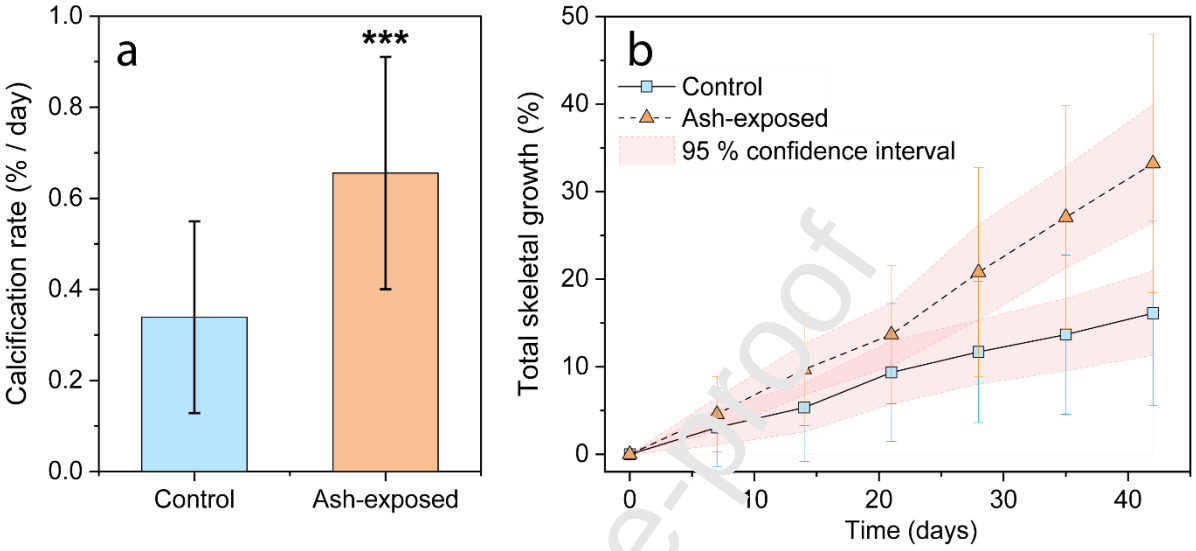

Figure 7: Skeletal growth rate of *Stylophora pistillata* reared in the control condition (blue) and after 6 weeks of exposure to 250 mg volcanic ash L^{-1} $week^{-1}$ (orange) (n = 21 per condition). An increase in skeletal mass is expressed as (a) calcification rate (% d^{-1}), and monitored as (b) total skeletal growth (%). Data is presented as mean ± SD. Statistically significant differences between treatments are represented by asterisks (*), with an indication of the level of significance in the number of asterisks.

3.3. Major and trace element content

3.3.1. Volcanic ash

The entire chemical characterization of major and trace elements of the volcanic ash is listed in Tab. A1. Based on its intermediate silica-content (55.87 ± 0.69 wt.% SiO_2) and total alkaline content (4.47 ± 0.07 wt.% Na_2O + K_2O) the volcanic ash can be assigned to the basaltic-andesitic rock composition. Other main oxide constituents are Al_2O_3 (19.11 ± 0.03 wt.%), CaO

(8.02 ± 0.06 wt.%), Fe_2O_3 (7.5 ± 0.33 wt.%), MgO (2.91 ± 0.01 wt.%) and MnO (0.15 ± 0.00 wt.%). Trace metal contents range from 0.19 ± 0.02 ppm Cd to 248.41 ± 53.39 ppm Zn. The ash contains high concentrations of metals in the order Zn (248 ppm) > Sr (202 ppm) > V (165.1 ppm) > Ba (129 ppm) > Cu (116.3 ppm).

3.3.2. Coral metallome

Within one condition (control or ash-exposed), the metal concentration (in ng cm^{-2}) in the host tissue is generally higher than in the symbionts (on average 4.5 ± 2.6 x higher; Tab.1), due to the higher biomass per skeletal surface area of the host compared to the symbionts. The largest difference was measured in the Co (~8x higher) and the Ni content (~9x higher) and the smallest difference in the Cr (~1.5x) concentration between coral tissue and symbionts of one condition. The six weeks exposure to volcanic ash influenced the metallome of coral host and its endosymbionts significantly. Of the ten measured transition metals (Tab. 1), seven were statistically significantly enriched in the ash-exposed coral tissue (Cr > Mn > Fe > Co > Cu > Zn > Ni) and three were enriched in the symbionts subjected to ash (Cr > Fe > Mn). The Cr concentration in tissue and symbionts was affected the most compared to the control samples (6.5x higher in ash-exposed tissue, WMW, $p < 0.003$; 4.7x higher in ash-exposed symbionts, WMW, $p < 0.003$), followed by changes in the Mn content for the coral tissue (4.2x higher, ANOVA, $p < 0.00004$) and Fe content in the dinoflagellates (3.4x higher, WMW, $p < 0.003$). The metal concentrations of V, Mo and Cd in the tissue are similar for both control and ash-exposed nubbins. Symbionts did not show a significant metal enrichment in V, Co, Ni, Cu, Zn, Mo and Cd upon ash-exposure.

Table 1: Trace metal concentration normalized to skeletal surface area [ng cm^{-2}] in the coral tissue and endosymbionts of *Stylophora pistillata* reared in a control condition and after 6 weeks of exposure to 250 mg volcanic ash L^{-1} $week^{-1}$ (n = 6 per condition). Normal distribution and homoskedasticity were assessed using Shapiro-Wilk test and Levene test, respectively. Based on former and latter outcome, statistical tests (ANOVA, WMW and Welch) were performed. Statistical results are presented as p-values.

Sample	**Element**	**Concentration** [ng cm^{-2}]		**Statistical test**		
		Control	*Ash-exposed*	*Type*	*p-value*	*Level of significance*
Coral host	V	3.47 (±2.61)	4.7 (±2.82)	WMW	0.394	
	Cr	0.43 (±0.16)	2.79 (±2.12)	WMW	0.002	**
	Mn	2.28 (±0.66)	9.72 (±2.52)	ANOVA	3.70E-05	***
	Fe	93.6 (±29.28)	221.34 (±56.24)	ANOVA	5.92E-04	***
	Co	0.67 (±0.24)	1.24 (±0.4)	ANOVA	0.014	*
	Ni	15.47(±2.99)	22.84 (±6.9)	ANOVA	0.037	*
	Cu	25.78 (±6.44)	44.33 (±14.25)	ANOVA	0.016	*
	Zn	279.83 (±71.94)	469.41 (±119.69)	ANOVA	0.008	**
	Mo	1.88 (±0.45)	1.9 (±0.31)	ANOVA	0.937	
	Cd	0.693 (±0.13)	0.85 (±0.15)	ANOVA	0.142	
Symbionts	V	0.7 (±0.33)	1.12 (±0.38)	ANOVA	0.070	
	Cr	0.29 (±0.07)	1.35 (±0.58)	WMW	0.002	**
	Mn	0.81 (±0.4)	2.1 (±0.61)	ANOVA	0.001	**
	Fe	31.81 (±7.42)	109.67 (±32.43)	WMW	0.002	**
	Co	0.09 (±0.02)	0.14 (±0.06)	WMW	0.132	
	Ni	1.99 (±0.7)	2.75 (±0.83)	ANOVA	0.114	
	Cu	8.59 (±2.63)	12.29 (±4.32)	ANOVA	0.103	
	Zn	115.89 (±39.83)	161.84 (±36.84)	ANOVA	0.065	

Mo	0.42 (±0.12)	0.43 (±0.15)	ANOVA	0.856
Cd	0.42 (±0.11)	0.50	ANOVA	0.619

p-value > 0.05 (not significant), p-value ≤ 0.05 (*) p-value ≤ 0.01 (**), and p-value ≤ 0.001 (***).
Data is presented as mean concentration ± SD.

4. Discussion

The effect of volcanic ash on coral physiology could be quantified since experimental conditions such as light intensity, ambient temperature, and pH did not change notably throughout the study. Volcanic ash supplied the coral with important micronutrients, altering the metallome of the coral holobiont, with an increased accumulation of essential metals (especially Cr, Fe and Mn; Tab. 1). Exposure to volcanic ash induced significant changes in the fluorescence-derived photochemical parameters (Φ_{PSII}, F_v/F_m, NPQ, rETR; Fig. 5 & 6) and photosynthetic reactions, directly enhancing symbiont photosynthesis (P_g, P_n; Fig. 4). In *Stylophora pistillata* translocated photosynthates account for up to 95 % of the daily requirements for respiration and growth (Muscatine et al., 1984; Muscatine, 1990). Consequently, the enhancement in photosynthesis observed in the ash-exposed nubbins, resulted in a higher energy budget for host metabolism that manifested in an elevated skeletal growth rate (Fig. 7). The beneficial role of volcanic ash exposure is supported by the fact that neither photophysiological stress nor signs of lipid peroxidation (equal MDA levels) (Fig. A3) or protein damage could be detected (Fig. 3b). In addition, the metabolic demand of the coral host (based on respiration; Fig. 4a) did not differ between conditions.

4.1. Volcanic ash supplies essential metals to the coral holobiont

Upon contact with seawater, pristine volcanic ash is reported to release large amounts of major and trace metals (Frogner et al. 2001; Jones and Gislason, 2008). Flow-through experiments report a high initial discharge of elements into the surrounding water within the first hour with reducing contributions over longer timescales (Frogner et al., 2001; Wygel et al., 2019). This indicates the rapid dissolution of metal salts (Jones and Gislason, 2008) and fast ash surface reactions, instantaneously supplying bioavailable key nutrients to the coral. There are several mechanisms by which corals can regulate the increased metal availability from ash-leaching: (i) storage in tissue and symbionts (as seen in Fig. 8); (ii) metal binding to proteins such as glutathione (Mitchelmore et al., 2007); and (iii) the expulsion of the Symbiodiniaceae (= coral bleaching), which has been reported as a stress response to metal loading (Meehan and Ostrander, 1997; Peters et al., 1997).

Volcanic ash leaching supplied the coral *S. pistillata* with an excess amount of trace metals, which were incorporated in both tissue and symbionts (Tab. 1, Fig. 8a). Transition metals (Cr, Mn, Co, Ni, Zn and Cd) preferentially accumulated in the host tissue (Fig. 8b), with the exception of iron, which showed a higher relative enrichment in the dinoflagellates. The increased accumulation of Fe in the symbionts was also measured in a comparative study conducted by Blanckaert et al. (2022), in which nubbins of *S. pistillata* were exposed to 5 mg L^{-1} $week^{-1}$ of desert dust. The results showcase that even the addition of small amount of dust can have significant changes in the metal uptake of coral host and dinoflagellates (Fig. 8b). Although, the enrichment of biological essential metals in coral tissue and symbionts is also noticeable in other studies (Anu et al., 2007; Chan et al., 2014), there is evidence that coral tissue does not accumulate high metal concentrations, in contrast to other invertebrates in a contaminated area (Brown and Holley, 1982). In laboratory settings, a rapid metal uptake was observed in coral tissue and Symbiodiniaceae as a response to metal loadings (Metian et al.,

2015; Blanckaert et al., 2022), although the incorporation is not systematic between the two tissue types. Many studies report that the metal-specific uptake in symbionts is greater than in coral tissues (Harland et al., 1990; Reichelt-Brushett and McOrist, 2003; Ranjbar Jafarabadi et al., 2018; Blanckaert et al., 2022), indicating that the symbionts play an important role in the uptake and accumulation of trace metals in their organism.

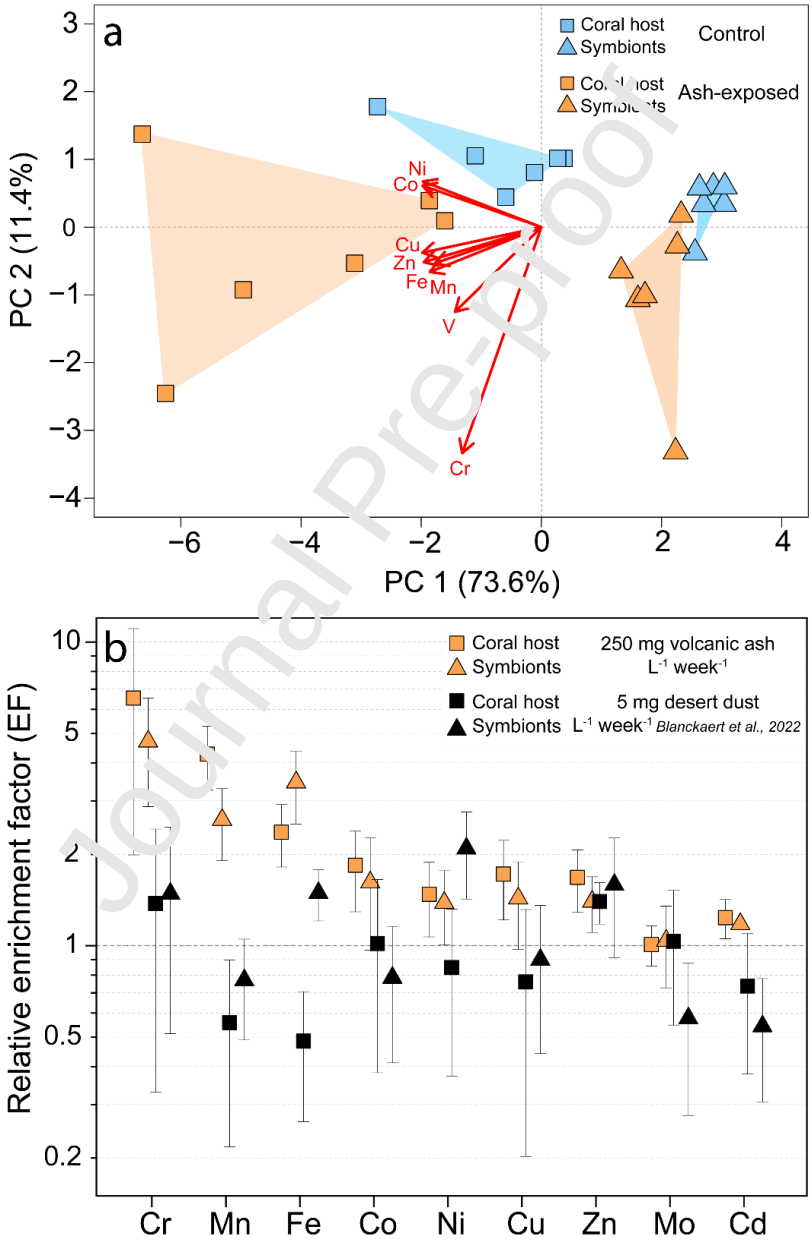

Figure 8: Trace metal content of coral tissue and symbionts normalized to skeletal surface area of *Stylophora pistillata* after the exposure experiment. (a) Principal component analysis (PCA) of the

metal content in coral host and Symbiodiniaceae of *Stylophora pistillata* reared in the control (blue) and after 6 weeks of exposure to 250 mg volcanic ash L^{-1} $week^{-1}$ (orange) (n = 6 per condition). (b) Relative enrichment factor (rEF) of coral host and Symbiodiniaceae of *Stylophora pistillata* exposed to volcanic ash (orange) and desert dust (black) *(Blanckaert et al., 2022)*. rEF is calculated as $conc._{Ash\text{-}exposed}$ [ng cm^{-2}] / mean $conc._{Control}$ [ng cm^{-2}]. rEF > 1 = enriched in ash-exposed nubbins, rEF < 1 = enriched in control nubbins. Data is presented as mean ± SD.

4.2. Positive photophysiological response of the coral to volcanic ash

Many of the enriched elements in coral host and symbionts (Tab 1, Fig. 8a) are important metallocofactors in proteins or protein complexes participating in various biochemical pathways and molecular processes in the Symbiodiniaceae (Reich et al., 2020). In addition, metals support fundamental cell functions and cellular responses to physiological stress. In cases where one metal is limiting (Twining and Baines, 2013), a mutualistic process is constituted, which helps maintain enzymatic activities (Blaby-Haas and Merchant, 2012; Rodriguez et al., 2016; Reich et al., 2020).

Photosynthetically active organisms have several metal requirements. For example, Co is incorporated into vitamin B_{12} (Croft et al., 2005) and Mo is an important metallocofactor of nitrogenase (Seefeldt et al., 2009). Symbiodiniaceae have also an absolute Fe and Mn requirement resulting from the non-substitutable role of these metals as electron transporters in the light-dependent reactions in the thylakoid membrane (Raven et al., 1999; Morel and Price, 2003). In particular, Fe is involved in the composition of cytochrome b_6f and ferrodoxin complexes (Raven et al., 1999), while Mn is a co-limiting factor of photosynthesis (Biscéré et al., 2018a) as it is a cofactor in the oxygen-evolving complex (OEC) of PS II (Ghanotakis and Yocum, 1990) and essential in chlorophyll biosynthesis *via* the isoprenoid biosynthetic pathway (Millaleo et al., 2010). Simultaneous Fe-Mn supplementation to *S.*

pistillata in aquaria experiments led to an improved photo-physiological response (Biscéré et al., 2018a). Photosynthetic yields of PSII of Symbiodiniaceae represent how effective light energy can be utilized by PSII to drive photosynthesis and thus support coral metabolism (Bhagooli et al., 2021). In our experiments, coral nubbins exposed to volcanic ash showed a rapid increase in photosynthetic efficiency (Φ_{PSII}) relative to the control nubbins after only 4 days, with a maximum value of ~0.5 in the effective quantum yield at the end of the experiment (Fig. 5). In the RLC, elevated values of F_v/F_m (~0.6) and relative electron transport rates rETR (~40 at PAR = 664) (Fig 6b & c, respectively), which are consistent with increased oxygen production (P_n and P_g; Fig 4), also indicate a positive physiological response in the ash-exposed nubbins relative to the control nubbins. Therefore, at similar experimental conditions (pH, temperature, salinity, and light intensity), the ash-exposed Symbiodiniaceae could harvest photon energy more efficiently than nubbins reared in the control condition. These observations, along with statistically significantly higher Fe and Mn concentrations of ash-exposed coral tissue (Fe, ANOVA, $p < 0.0006$; Mn, ANOVA, $p < 0.00004$) and symbionts (Fe, WMW, $p < 0.003$; Mn, ANOVA, $p < 0.001$), indicate that the observed positive physiological response is driven by a simultaneous Fe-Mn enrichment in ash-exposed samples (Tab. 1). Such high photosynthetic efficiency in ash exposed nubbins can be achieved thanks to higher concentrations of chlorophyll *a* and c_2 (Fig. 3c), which are the photopigments responsible for light capture (Green and Durnford, 1996). This is congruent to the (1.3 – fold) increase in the symbiont density upon ash exposure (Fig. 3a). Symbiodiniaceae have indeed a relatively high Fe requirement when compared to other microalgae and an increase in the Fe concentration is linked to an increased growth rate of the dinoflagellates in culture (Reich et al., 2020). This is consistent with the observation that the exposure of *S. pistillata* to solely Fe (6 nM Fe) led to increased symbiont densities, which were correlated to higher P_g and R

normalized per skeletal surface area (Ferrier-Pagès et al., 2001).

Control nubbins likely regulated the excess excitation energy by heat dissipation within the PSII reaction centres (Gorbunov et al., 2001), as reflected in the higher NPQ levels (Fig. 6d). In both conditions, NPQ levels rose with increasing irradiance, as this is the photoprotective effect of the xanthophyll cycle (Brown et al., 1999) to avoid damage to PSII at high light intensities. At low light intensities (PAR < 664) F_v/F_m and rETR levels were significantly higher in ash-exposed corals (Fig. 6b & d). At high light irradiance, levels of rETR and F_v/F_m nubbins were similar in control nubbins and ash-exposed, suggesting that volcanic ash exposure advanced light capture and light use at low light environments for *S. pistillata.* Persistent turbidity after ash addition could have altered F_v/F_m levels, as seen for sediment analogs (Junjie et al., 2014; Jones et al., 2022), but magnitude (a decrease of 28.48 ± 16 µmol photons m^{-2} s^{-1} irradiance; Fig. A2a) and duration (cleared 3-4h after ash addition) of the occurring turbidity is interpreted to be negligible. Nevertheless, the response of the ash-exposed nubbins at low-light intensity suggests that even with elevated turbidity in the water column the positive effects of volcanic ash may counteract the stresses induced by reduced insolation. At the physiological level, other metals (such as Ni, Zn and Cu) are also involved in the biochemical pathways of photosynthesis (Reich et al., 2020) and oxidative stress detoxification processes, potentially affecting photo-physiological parameters and increasing the corals resistance to thermal stress, and therefore coral bleaching (Ferrier-Pagès et al., 2018). For example, Cu and Zn are catalytic cofactors of the superoxide dismutase 1 (Cu-Zn SOD1), which, alongside the catalase and the glutathione peroxidase, is considered as the most efficient antioxidant enzymes that regulate oxidative stress through reactive oxygen species (ROS) scavenging (Finkel and Holbrook, 2000). Constant Ni exposure at ecologically relevant concentrations (3.5 µg L^{-1}) significantly increased chlorophyll *a* and c_2 content and P_g

of *S. pistillata* (Biscéré et al., 2018b). The increase in chlorophyll biomass is explained by the replacement of Mg with Ni in chlorophyll synthesis (Küpper et al., 1996). Furthermore, nubbins supplied with Ni at ambient temperature (25°C) increased long-term calcification rates (Biscéré et al., 2017; 2018b) in corals due to the activity of urease, which facilitates the breakdown of urea to produce inorganic carbon and ammonia.

Ultimately, volcanic ash supplies a mixture of limited essential bio-elements to the holobiont coral, stimulating the primary production of the endosymbiotic dinoflagellates. This suggests that subsequent biological growth will be limited by macronutrient availability (Jones and Gislason, 2008). The fertilizing effect of volcanic ash deposition, which was proven prior in the occurrence of phytoplankton blooms in ocean surface waters following ash deposition after a volcanic eruption (Uematsu et al., 2004; Hamme et al., 2010; Browning et al., 2015), can be expanded to the increased activity of Symbiodiniaceae.

4.3 Hormetic response to metal loadings and metal toxicity

Monitoring the effective quantum yield over time provides a time-resolved assessment of coral health, as decreasing Φ_{PSII} resembles an early signal of stress (Ralph et al., 2005; Kuzminov et al., 2013; Bellisanti et al., 2021). In our experiment, prolonged ash exposure steadily increased the photochemical efficiency of the symbionts (Fig. 5), indicating healthy corals throughout the experimental duration. Even though many elements are leached from volcanic ash and enriched in symbiont and coral tissue (Fig. 8a), there is no evidence that metal-specific toxic thresholds were reached in the applied experimental settings (Fig. A3). If a small concentration of a potential toxic element induces a beneficial response in the organism, then we speak of hormesis (Calabrese, 2008). For example, Co toxicity exists for *S. pistillata* above 1.06 ± 0.16 µg L^{-1}, which will lead to decreased skeletal growth and

photosynthetic rates (Biscéré et al., 2015). However, a small added concentration of Co (0.2 µg L^{-1}) is reported to stimulate photochemical reactions in *S. pistillata* with higher obtained values of rETR, although a simultaneous decrease in the skeleton growth rate was observed after 3 weeks (Biscéré et al., 2015). Common signs of metal poisoning are lipid peroxidation, as reactive oxygen species (ROS) production can be enhanced by metals (Shaw et al., 2004), the decrease in chlorophyll biomass (as seen for planktonic diatoms in Rijstenbil et al. (1994)), or coral bleaching. Coral bleaching is one detoxification mechanism to high metal loadings, which harms the coral and is an early precursor to coral death The threshold at which symbiotic algae are ejected varies not only between coral and symbiont species, as antioxidant capacities and oxidative stress prevention are clade-specific (Dal Pizzol et al., 2022), but it is also related to the tolerance of the coral to the specific metal. Tolerance can be built up through frequent exposure to the critical metal (Harland and Brown, 1989), which is an important factor for field studies. As we investigated the interaction of volcanic ash with corals reared in culture conditions at CSM, no previous metal loads are assumed. Corals exposed to volcanic ash, did not experience bleaching (Fig. 3a). On the contrary, we only measured a positive effect of volcanic ash exposure to the coral physiology.

Nevertheless, given the chemical complexity of volcanic ash, we cannot rule out the possibility that individual metals reached toxic levels in solution but this was outweighed by the positive effect of the "micronutrient-cocktail" provided by volcanic ash. The fitness of the holobiont coral was increased, pointing towards hormetic stimulation (Calabrese, 2008). The nutrient supplyof volcanic ash could be interpreted as a mechanism to help corals cope with external stress, similar to effects observed in previous experiments where Fe-Mn in solution (Biscéré et al., 2018a) and leached from natural desert dust (Blanckaert et al., 2022) increased coral

resistance to heat stress-induced bleaching. We did not purposely expose the nubbins to a specific stressor, such as heat, so this would need to be investigated in further experiments.

4.4. Translation and adaptation to field-based coral reef studies

Volcanic ash is an important source of Fe in Fe-limited regions of the ocean (Duggen et al., 2007, 2010; Olgun et al., 2011; Ayris and Delmelle, 2012) and most likely an important source of Mn too. Both global Fe and Mn cycles are hypothesized to be largely influenced by subaerial volcanism (Longman et al., 2022), increasing primary productivity (Frogner et al., 2001). Fe and Mn could also be linked to increased phytoplankton growth in open ocean settings (Browning et al., 2021). It is, to our knowledge, the first time that exposure to volcanic ash deposition has been observed to positively impact coral physiology. This is likely because the majority of studies are field-based and focused on proximal locations to volcanic eruptions, where smothering can lead to coral mortality (Heikoop et al., 1996; Vroom and Zgliczynski, 2011; Schils, 2012; Wu et al., 2018). Nevertheless, the energy gain from photosynthesis we have observed in our experiments, which results from metal leaching in ambient seawater or *in situ* within the organism after ingestion, could be excreted in the form of coral mucus (Xu et al., 2022) as it is a protective mechanism against sedimentation stress (reviewed in Brown and Bythell, 2005). This may explain the rapid recovery of reefs in close proximity to volcanic eruptions (Smallhorn-West et al., 2020), improving their resilience to these extreme events. In our experiments, coral nubbins did not experience smothering or high levels of turbidity, allowing the additional energy to be used for biomineralization and is observed with sustained skeletal growth weeks after constant ash addition. Even if an energy gain can be used for biomineralization, it may lead to growth defects as observed by McKnight et al. (1981), who reported an increased growth rate of an algal population upon a dilute tephra deposition. It

is important to recognize that the observed effects upon ash-exposure are only valid for the selected experimental parameters (e.g., distinct volcanic ash, coral species, amount, and frequency of added ash). Volcanic ash from different sources leaches different metals in varying concentrations (Ayris & Delmelle, 2012; Wygel et al., 2019), which might induce similar hormetic effects, but could also be leached above a toxic threshold and thus be detrimental, and so the response we observed may not be universally global for all volcanic eruptions.

Transferring the results to the field is a substantial goal, but for this, a proper understanding of the general conditions of a coral reef ecosystem and its biodiversity in the aftermath of a volcanic eruption is needed. Volcanogenic metal discharge might be a major contributor for element cycling in ocean biogeochemistry (Longman et al., 2022), affecting coral reef physiology. To understand the biogeochemical response of coastal coral reefs to dilute ash-exposure we can draw parallels with the island mass effect (IME; first established by Doty and Oguri (1956)). The IME describes the abundance and high productivity levels in phytoplankton biomass in the proximity to an island-reef ecosystem compared to oligotrophic oceanic conditions. Both geological factors (e.g., groundwater discharge, terrestrial and river runoff, geomorphic type and steepness of the slope (Gove et al., 2016; Reich et al., 2023)), and biotic factors (e.g., seabird or fish feces (Savage, 2019; Van Wert et al., 2023)) lead to a local nutrient enrichment at continental margins. A higher nutrient flux will lead to increased plankton densities (Hallock and Schlager, 1986) stimulating coral heterotrophy (i.e. capture of zooplankton by coral host). Heterotrophic feeding was proven to significantly enhance micronutrient concentrations in coral host and dinoflagellates (Ferrier-Pagès et al., 2018), increasing the corals resistance to thermal stress (Fox et al., 2023), and therefore prevent coral bleaching. Given the positive photo physiological and hormetic responses to metal

loading from volcanic ash observed in our experiments, we suggest fertilization through ash leaching is an example of another process that will increase the micronutrient budget at a reef scale, with similar consequences as observed for the IME.

Whilst increasing the micronutrient supplementation will stimulate coral heterotrophy (Fox et al., 2023), leading to a species-specific benefits on a coral reef scale, we cannot expect such a process to be universal for all volcanic eruptions across all spatial scales. From a volcanology perspective, the frequency and duration of explosive events will vary between eruptions (Druitt et al., 2002; Cole et al., 2023), the composition of the erupted material (Armienta et al., 2002) and also the scale and geographic locality of deposition (Longman et al., 2022) can vary, all of which will lead to variations in the elements and magnitude of their leaching. From an ecophysiological perspective, coral smothering will occur where ash loadings are high (Eldredge and Kropp, 1985; Ono et al., 2007; Vroom and Zgliczynski, 2011; Wu et al., 2018), although this can be somewhat counteracted by the additional energy budget associated with micronutrient leaching, as we have observed in this study. Additionally, there is a risk that volcanic ash provides an oversupply of micronutrients leading to increased food supply and resulting in reduced water transparency and elevated levels of interspecific benthic competition (Hallock and Schlager, 1986; D'Angelo and Wiedenmann, 2014). Consequently, for any future work it will be important to investigate at what magnitudes of ash-loading a transition occurs between these possible negative impacts to the positive impacts we have observed in our study.

5. Conclusion

Explosive volcanic eruptions are capable of generating large volumes of tephra (10^{11}-10^{15} kg of released magma (Self, 2006)), disrupting all ecosystems in their vicinity and influencing biogeochemical cycles globally. Studies reporting on the effect of volcanic ash deposition on coral reefs are scarce and commonly report mass mortality (Heikoop et al., 1996; Vroom and Zgliczynski, 2011; Schils, 2012; Wu et al., 2018) of large portions of the coral reef close to the volcano. Information about the physiological response of corals to volcanic ash has not been gathered yet.

In this study, we conclude that dilute concentrations of volcanic ash, deposited 10's – 100's km from a source volcano, can have a beneficial effect on the photosynthetic apparatus of the symbionts in *Stylophora pistillata*, grown under controlled culture conditions. Volcanic ash leaches essential biometals into the ambient seawater, which are accumulated in the coral tissue and symbionts, supporting the primary production of the symbionts. The known fertilizing effect of freshly erupted ash (Frogner et al., 2001; Jones and Gislason, 2008) was observed for the first time for coral holobiont activity. The beneficial role of volcanic ash leaching to the symbiont activity is evident days after initiating ash supply, with an increase in photochemical efficiency of PSII of the symbionts, which supplies the coral host with an additional input of energy. Volcanic ash exposure has short-term and longer-lasting advantageous effects on coral metabolism, and additionally, energy can be used for biomineralization. However, whilst an increase in Φ_{PSII} was observed soon after the beginning of the experiment, a significant difference in the skeletal growth rate was only evident after weeks of prolonged ash supply. The addition of the volcanic ash in this study at a given concentration did not stress the coral, suggesting the supply of micronutrients through volcanic ash leaching yields the potential to counterbalance external stresses such as those induced by climate change.

Acknowledgments

The authors are grateful for the laboratory assistance from Maria-Isabelle Marcus, Romie Tignat-Perrier, and Alice Blanckaert at the Centre Scientifique de Monaco (Monaco). Eric Béraud (Centre Scientifique de Monaco) helped with the interpretation of the chlorophyll fluorescence data. We acknowledge John B. Mwansa (Barbados Water Authority) for collecting and providing the volcanic ash samples. Last but not least, the authors would like to thank the reviewers for expanding the scope of this paper and helped us improving the quality of the manuscript. This work was funded by the Swiss National Science Foundation (project PCEFP2_194204).

References

Anu, G., Kumar, N.C., Jayalakshmi, K.., Nair, S.M., 2007. Monitoring of heavy metal partitioning in reef corals of Lakshadweep Archipelago, Indian Ocean. Environ. Monit. Assess. 128, 195–208. https://doi.org/10.1007/s10661-006-9305-7

Armienta, M.A., De la Cruz-Reyna, S., Morton, O., Cruz, O., Ceniceros, N., 2002. Chemical variations of tephra-fall deposit leachates for three eruptions from Popocatépetl volcano. J. Volcanol. Geotherm. Res. 117, 61–80. https://doi.org/10.1016/S0377-0273(01)00251-7

Ayris, P.M., Delmelle, P., 2012. The immediate environmental effects of tephra emission. Bull. Volcanol. 74, 1905–1936. https://doi.org/10.1007/s00445-012-0654-5

Bhagooli, R., Mattan-Moorgawa, S., Kaullysing, D., Louis, Y.D., Gopeechund, A., Ramah, S., Soondur, M., Pilly, S.S., Beesoo, R., Wijayanti, D.P., Bachok, Z.B., Monrás, V.C., Casareto, B.E., Suzuki, Y., Baker, A.C., 2021. Chlorophyll fluorescence – A tool to assess photosynthetic performance and stress photophysiology in symbiotic marine invertebrates and seaplants. Mar. Pollut. Bull. 165, 112059. https://doi.org/10.1016/j.marpolbul.2021.112059

Bilger, W., Björkman, O., 1990. Role of the xanthophyll cycle in photoprotection elucidated by measurements of light-induced absorbance changes, fluorescence and photosynthesis in leaves of Hedera canariensis. Photosynth. Res. 25, 173–185. https://doi.org/10.1007/BF00033159

Birkeland, C., 1976. An experimental method of studying corals during early stages of growth. Micronesica 12, 319–322.

Biscéré, T, Ferrier-Pagès, C., Gilbert, A., Pichler, T., Houlbrèque, F., 2018a. Evidence for mitigation of coral bleaching by manganese. Sci. Rep. 8. https://doi.org/10.1038/s41598-018-34994-4

Biscéré, T., Ferrier-Pagès, C., Grover, R., Gilbert, A., Rottier, C., Wright, A., Payri, C., Houlbrèque, F., 2018b. Enhancement of coral calcification via the interplay of nickel and urease. Aquat. Toxicol. 200, 247–256. https://doi.org/10.1016/j.aquatox.2018.05.013

Biscéré, T., Lorrain, A., Rodolfo-Metalpa, R., Gilbert, A., Wright, A., Devissi, C., Peignon, C., Farman, R., Duvieilbourg, E., Payri, C., Houlbrèque, F., 2017. Nickel and ocean warming affect scleractinian coral growth. Mar. Pollut. Bull. 120, 250–258. https://doi.org/10.1016/j.marpolbul.2017.05.025

Biscéré, T., Rodolfo-Metalpa, R., Lorrain, A., Chauvaud, L., Thébault, J., Clavier, J., Houlbrèque, F., 2015. Responses of Two Scleractinian Corals to Cobalt Pollution and Ocean Acidification. PLOS ONE 10, e0122898. https://doi.org/10.1371/journal.pone.0122898

Blaby-Haas, C.E., Merchant, S.S., 2012. The ins and outs of algal metal transport. Cell Biol. Met. 1823, 1531–1552. https://doi.org/10.1016/j.bbamcr.2012.04.010

Blanckaert, A.C.A., Omanović, D., Fine, M., Grover, R., Ferrier-Pagès, C., 2022. Desert dust deposition supplies essential bioelements to Red Sea corals. Glob. Change Biol. 28, 2341–2359. https://doi.org/10.1111/gcb.16074

Blong, R.J., 1984. Volcanic hazards. A sourcebook on the effects of eruptions. Academic Press, Inc.,Orlando, FL, United States.

Bradford, M.M., 1976. A Rapid and Sensitive Method for the Quantitation of Microgram Quantities of Protein Utilizing the Principle of Protein-Dye Binding.

Brown, B., Bythell, J., 2005. Perspectives on mucus secretion in reef corals. Mar. Ecol. Prog. Ser. 296, 291–309. https://doi.org/10.3354/meps296291

Brown, B.E., Ambarsari, I., Warner, M.E., Fitt, W.K., Dunne, R.P., Gibb, S.W., Cummings, D.G., 1999. Diurnal changes in photochemical efficiency and xanthophyll concentrations in shallow water reef corals : evidence for photoinhibition and photoprotection. Coral Reefs 18, 99–105. https://doi.org/10.1007/s003380050163

Brown, B.E., Holley, M.C., 1982. Metal levels associated with tin dredging and smelting and their effect upon intertidal reef flats at ko phuket, Thailand. Coral Reefs 1, 131–137. https://doi.org/10.1007/BF00301655

Browning, T.J., Achterberg, E.P., Engel, A., Mawji, E., 2021. Manganese co-limitation of phytoplankton growth and major nutrient drawdown in the Southern Ocean. Nat. Commun. 12, 884. https://doi.org/10.1038/s41467-021-21122-6

Browning, T.J., Stone, K., Bouman, H.A., Mather, T.A., Pyle, D.M., Moore, C.M., Martinez-Vicente, V., 2015. Volcanic ash supply to the surface ocean-remote sensing of biological responses and their wider biogeochemical significance. Front. Mar. Sci. 2. https://doi.org/10.3389/fmars.2015.00014

Calabrese, E.J., 2008. Hormesis: why it is important to toxicology and toxicologists. Environ. Toxicol. Chem. 27, 1451. https://doi.org/10.1897/07-541.1

Chan, I., Hung, J.J., Peng, S.H., Tseng, L.C., Ho, T.Y., Hwang, J.S., 2014. Comparison of metal accumulation in the azooxanthellate scleractinian coral (Tubastraea coccinea) from different polluted environments. Mar. Pollut. Bull. 85, 648–658. https://doi.org/10.1016/j.marpolbul.2013.11.015

Cole, P.D., Barclay, J., Robertson, R.E.A., Mitchell, S., Davies, B.V., Constantinescu, R., Sparks, R.S.J., Aspinall, W., Stinton, A., 2023. Explosive sequence of La Soufrière, St Vincent, April 2021: insights into drivers and consequences via eruptive products. Geol. Soc. Lond. Spec. Publ. 539, SP539-2022–292. https://doi.org/10.1144/SP539-2022-292

Croft, M.T., Lawrence, A.D., Raux-Deery, E., Warren, M.J., Smith, A.G., 2005. Algae acquire vitamin B12 through a symbiotic relationship with bacteria. Nature 438, 90–93. https://doi.org/10.1038/nature04056

Dal Pizzol, J.L., Marques, J.A., da Silva Fonseca, J., Costa, P.G., Bianchini, A., 2022. Metal accumulation induces oxidative stress and alters carbonic anhydrase activity in corals and

symbionts from the largest reef complex in the South Atlantic ocean. Chemosphere 290, 133216. https://doi.org/10.1016/j.chemosphere.2021.133216

D'Angelo, C., Wiedenmann, J., 2014. Impacts of nutrient enrichment on coral reefs: New perspectives and implications for coastal management and reef survival. Curr. Opin. Environ. Sustain. 7, 82–93. https://doi.org/10.1016/j.cosust.2013.11.029

Dellisanti, W., Chung, J.T.H., Chow, C.F.Y., Wu, J., Wells, M.L., Chan, L.L., 2021. Experimental Techniques to Assess Coral Physiology in situ Under Global and Local Stressors: Current Approaches and Novel Insights. Front. Physiol. 12, 656562. https://doi.org/10.3389/fphys.2021.656562

Doty, M.S., Oguri, M., 1956. The Island Mass Effect. ICES J. Mar. Sci. 22, 33–37. https://doi.org/10.1093/icesjms/22.1.33

Druitt, T.H., Young, S.R., Baptie, B., Bonadonna, C., Calder, E.S., Clarke, A.B., Cole, P.D., Harford, C.L., Herd, R.A., Luckett, R., Ryan, G., Voight, B., 2002. Episodes of cyclic Vulcanian explosive activity with fountain collapse at Soufrière Hills Volcano, Montserrat. Geol. Soc. Lond. Mem. 21, 281–306. https://doi.org/10.1144/GSL.MEM.2002.021.01.13

Duggen, S., Croot, P., Schacht, U., Hoffmann, L., 2007a. Subduction zone volcanic ash can fertilize the surface ocean and stimulate phytoplankton growth: Evidence from biogeochemical experiments and satellite data. Geophys. Res. Lett. 34. https://doi.org/10.1029/2006GL027522

Duggen, S., Croot, P., Schacht, U., Hoffmann, L., 2007b. Subduction zone volcanic ash can fertilize the surface ocean and stimulate phytoplankton growth: Evidence from biogeochemical experiments and satellite data. Geophys. Res. Lett. 34, L01612. https://doi.org/10.1029/2006GL027522

Duggen, S., Olgun, N., Croot, P., Hoffmann, L., Dietze, H., Delmelle, P., Teschner, C., Skolen, A.P.M., 2010. The role of airborne volcanic ash for the surface ocean biogeochemical iron-cycle: a review, Biogeosciences.

Eldredge, L.C., Kropp, R.K., 1985. Volcanic ashfall effects on intertidal and shallow-water coral reef zones at Pagan (Mariana Islands): Proceedings of the Fifth International Coral Reef Congress. Tahiti.

Ferrier-Pagès, C., Houlbrèque, F., Wyss, E., Richard, C., Allemand, D., Boisson, F., 2005. Bioaccumulation of zinc in the scleractinian coral Stylophora pistillata. Coral Reefs 24, 636–645. https://doi.org/10.1007/s00338-005-0045-x

Ferrier-Pagès, C., Sauzéat, L., Balter, V., 2018. Coral bleaching is linked to the capacity of the animal host to supply essential metals to the symbionts. Glob. Change Biol. 24, 3145–3157. https://doi.org/10.1111/gcb.14141

Ferrier-Pagès, C., Schoelzke, V., Jaubert, J., Muscatine, L., Hoegh-Guldberg, O., 2001. Response of a scleractinian coral, Stylophora pistillata, to iron and nitrate enrichment. J. Exp. Mar. Biol. Ecol. 259, 249–261. https://doi.org/10.1016/S0022-0981(01)00241-6

Ferrier-Pagès, C., Witting, J., Tambutté, E., Sebens, K.P., 2003. Effect of natural zooplankton feeding on the tissue and skeletal growth of the scleractinian coral Stylophora pistillata. Coral Reefs 22, 229–240. https://doi.org/10.1007/s00338-003-0312-7

Finkel, T., Holbrook, N.J., 2000. Oxidants, oxidative stress and the biology of ageing. Nature 408, 239–247. https://doi.org/10.1038/35041687

Fox, M.D., Guillaume-Castel, R., Edwards, C.B., Glanz, J., Gove, J.M., Green, J.A.M., Juhlin, E., Smith, J.E., Williams, G.J., 2023. Ocean currents magnify upwelling and deliver nutritional subsidies to reef-building corals during El Niño heatwaves. Sci. Adv. 9, eadd5032. https://doi.org/10.1126/sciadv.add5032

Franklin, L.A., Badger, M.R., 2001. A comparison of photosynthetic electron transport rates in macroalgae measured by pulse amplitude modulated chlorophyll fluorometry and mass spectrometry. J. Phycol. 37, 756–767. https://doi.org/10.1046/j.1529-8817.2001.00156.x

Frenzel, P., 1983. Effects of volcanic ash on the benthic environment of a mountain stream, northern Idaho. https://doi.org/10.3133/wri824106

Frogner, P., Gíslason, S.R., Óskarsson, N., 2001. Fertilizing potential of volcanic ash in ocean surface water. Geology 29, 487–490. https://doi.org/10.1130/0091-7613(2001)029<0487:FPOVAI>2.0.CO;2

Genty, B., Briantais, J.-M., Baker, N.R., 1989. The relationship between the quantum yield of photosynthetic electron transport and quenching of chlorophyll fluorescence. Biochim. Biophys. Acta BBA - Gen. Subj. 990, 87–92. https://doi.org/10.1016/S0304-4165(89)80016-9

Ghanotakis, D.F., Yocum, C.F., 1990. Photosystem II and the Oxygen-Evolving Complex. Annu. Rev. Plant Physiol. Plant Mol. Biol. 41, 255–276. https://doi.org/10.1146/annurev.pp.41.060190.001351

Gorbunov, M., Kolber, Z., Lesser, M., Falkowski, P., 2001. Photosynthesis and photoprotection in symbiotic corals. Limnol. Oceanogr. - LIMNOL Ocean. 46, 75–85. https://doi.org/10.4319/lo.2001.46.1.0075

Gove, J.M., McManus, M.A., Neuheimer, A.B., Polovina, J.J., Drazen, J.C., Smith, C.R., Merrifield, M.A., Friedlander, A.M., Ehses, J.S., Young, C.W., Dillon, A.K., Williams, G.J., 2016. Near-island biological hotspots in barren ocean basins. Nat. Commun. 7, 10581. https://doi.org/10.1038/ncomms10581

Green, B.R., Durnford, D.G., 1996. The chlorophyll-carotenoid proteins of oxygenic photosynthesis. Annu. Rev. Plant Physiol. Plant Mol. Biol. 47, 685–714. https://doi.org/10.1146/annurev.arplant.47.1.685

Hallock, P., Schlager, W., 1986. Nutrient Excess and the Demise of Coral Reefs and Carbonate Platforms. PALAIOS 1, 389. https://doi.org/10.2307/3514476

Hamme, R.C., Webley, P.W., Crawford, W.R., Whitney, F.A., DeGrandpre, M.D., Emerson, S.R., Eriksen, C.C., Giesbrecht, K.E., Gower, J.F.R., Kavanaugh, M.T., Peña, M.A., Sabine, C.L., Batten, S.D., Coogan, L.A., Grundle, D.S., Lockwood, D., 2010. Volcanic ash fuels anomalous plankton bloom in subarctic northeast Pacific: ASH FUELS ANOMALOUS PLANKTON BLOOM. Geophys. Res. Lett. 37, n/a-n/a. https://doi.org/10.1029/2010GL044629

Harland, A.D., Brown, B.E., 1989. Metal tolerance in the scleractinian coral Porites lutea. Pollut. Far East 20, 353–357. https://doi.org/10.1016/0025-326X(89)90159-8

Harland, A.D., Bryan, G.W., Brown, B.E., 1990. Zinc and cadmium absorption in the symbiotic anemone Anemonia viridis and the non-symbiotic anemone Actinia equina. J. Mar. Biol. Assoc. U. K. 70, 789–802. https://doi.org/10.1017/S0025315400059063

Heikoop, J.M., Tsujita, C.J., Risk, M.J., 1996. Corals as proxy recorders of volcanic activity: Evidence from Banda Api, Indonesia, Tomascik Source: PALAIOS.

Hoegh-Guldberg, O., Bruno, J.F., 2010. The Impact of Climate Change on the World's Marine Ecosystems. Science 328, 1523–1528. https://doi.org/10.1126/science.1189930

Hoffmann, L., Breitbarth, E., Boyd, P., Hunter, K., 2012. Influence of ocean warming and acidification on trace metal biogeochemistry. Mar. Ecol. Prog. Ser. 470, 191–205. https://doi.org/10.3354/meps10082

Hoogenboom, M.O., Campbell, D.A., Beraud, E., DeZeeuw, K., Ferrier-Pagès, C., 2012. Effects of Light, Food Availability and Temperature Stress on the Function of Photosystem II and Photosystem I of Coral Symbionts. PLoS ONE 7, e30167. https://doi.org/10.1371/journal.pone.0030167

Horwell C. J., Damby D. E., Stewart C., Joseph E. P., Barclay J., Davies B. V., Mangler M. F., Marvin L. G., Najorka J., Peek S., Tunstall N., 2023. Physicochemical hazard assessment of ash and dome rock from the 2021 eruption of La Soufrière, St Vincent, for the assessment of respiratory health impacts and water contamination. Geol. Soc. Lond. Spec. Publ. 539, SP539-2023–46. https://doi.org/10.1144/SP539-2023-46

Houk, P. (Ed.), 2011. Volcanic Disturbances and Coral Reefs, in: Encyclopedia of Modern Coral Reefs: Structure, Form and Process, Encyclopedia of Earth Sciences Series. Springer Netherlands, Dordrecht. https://doi.org/10.1007/978-90-481-2639-2

Howard, L., Brown, B., 1984. Heavy metals and reef corals. Oceanogr. Mar. Biol. Annu. Rev. 22, 192–208.

Hughes, T.P., Baird, A.H., Bellwood, D.R., Card, M., Connolly, S.R., Folke, C., Grosberg, R., Hoegh-Guldberg, O., Jackson, J.B.C., Kleypas, J., Lough, J.M., Marshall, P., Nyström, M., Palumbi, S.R., Pandolfi, J.M., Rosen, B., Roughgarden, J., 2003. Climate Change, Human Impacts, and the Resilience of Coral Reefs. Science 301, 929–933. https://doi.org/10.1126/science.1085046

Inman, D.L., 1952. Measures for describing the size distribution of sediments. J. Sediment. Petrol. 19, 125–145. https://doi.org/DOI 10.1306/D42694DB-2B26-11D7-8648000102C1865D

Jeffrey, S.W., Humphrey, G.F., 1975. New spectrophotometric equations for determining chlorophylls a, b, c1 and c2 in higher plants, algae and natural phytoplankton. Biochem. Physiol. Pflanz. 167, 191–194. https://doi.org/10.1016/s0015-3796(17)30778-3

Jokiel, P.L., Maragos, J.E., Franzisket, L., 1978. Coral growth: buoyant weight technique, in: Coral Reef: Research Methods, UNESCO. Paris, pp. 379–396.

Jones, L.A., Mannion, P.D., Farnsworth, A., Bragg, F., Lunt, D.J., 2022. Climatic and tectonic drivers shaped the tropical distribution of coral reefs. Nat. Commun. 13, 3120. https://doi.org/10.1038/s41467-022-30793-8

Jones, M.T., Gislason, S.R., 2008. Rapid releases of metal salts and nutrients following the deposition of volcanic ash into aqueous environments. Geochim. Cosmochim. Acta 72, 3661–3680. https://doi.org/10.1016/j.gca.2008.05.030

Joseph, E.P., Camejo-Harry, M., Christopher, T., Contreras-Arratia, R., Edwards, S., Graham, O., Johnson, M., Juman, A., Latchman, J.L., Lynch, L., Miller, V.L., Papadopoulos, I., Pascal, K., Robertson, R., Ryan, G.A., Stinton, A., Grandin, R., Hamling, I., Jo, M.-J., Barclay, J., Cole, P., Davies, B.V., Sparks, R.S.J., 2022. Responding to eruptive transitions during the 2020–2021 eruption of La Soufrière volcano, St. Vincent. Nat. Commun. 13, 4129. https://doi.org/10.1038/s41467-022-31901-4

Junjie, R.K., Browne, N.K., Erftemeijer, P.L.A., Todd, P.A., 2014. Impacts of sediments on coral energetics: Partitioning the effects of turbidity and settling particles. PLoS ONE 9. https://doi.org/10.1371/journal.pone.0107195

Kandlbauer, J., Carey, S.N., Sparks, R.S.J., 2013. The 1815 Tambora ash fall: implications for transport and deposition of distal ash on land and in the deep sea. Bull. Volcanol. 75, 708. https://doi.org/10.1007/s00445-013-0708-3

Küpper, H., Küpper, F., Spiller, M., 1996. Environmental relevance of heavy metal-substituted chlorophylls using the example of water plants. J. Exp. Bot. 47, 259–266. https://doi.org/10.1093/jxb/47.2.259

Kuzminov, F.I., Brown, C.M., Fadeev, V.V., Gorbunov, M.Y., 2013. Effects of metal toxicity on photosynthetic processes in coral symbionts, Symbiodinium spp. J. Exp. Mar. Biol. Ecol. 446, 216–227. https://doi.org/10.1016/j.jembe.2013.05.017

LaJeunesse, T.C., Parkinson, J.E., Gabrielson, P.W., Jeong, H.J., Reimer, J.D., Voolstra, C.R., Santos, S.R., 2018. Systematic Revision of Symbiodiniaceae Highlights the Antiquity and Diversity of Coral Endosymbionts. Curr. Biol. 28, 2570-2580.e6. https://doi.org/10.1016/j.cub.2018.07.008

Lee, D.B., 1996. Effects of the eruptions of Mount St. Helens on physical, chemical, and biological characteristics of surface water, ground water, and precipitation in the Western United States (Report No. 2438), Water Supply Paper. United States Geological Survey. https://doi.org/10.3133/wsp2438

Lewis, J.B., 1960. The coral reefs and coral communities of Barbados, W.I. Can. J. Zool. 38, 1133–1145. https://doi.org/10.1139/z60-118

Longman, J., Palmer, M.R., Gernon, T.M., Manners, H.R., Jones, M.T., 2022. Subaerial volcanism is a potentially major contributor to oceanic iron and manganese cycles. Commun. Earth Environ. 3, 60. https://doi.org/10.1038/s43247-022-00389-7

Macdonald, R., Hawkesworth, C.J., Heath, E., 2000. The Lesser Antilles volcanic chain: a study in arc magmatism. Earth-Sci. Rev. 49, 1–76. https://doi.org/10.1016/S0012-8252(99)00069-0

McKnight, D.M., Feder, G.L., Stiles, E.A., 1981. Toxicity of Volcanic-Ash Leachate to a Blue-Green Alga. Results Of A Preliminary Bioassay Experiment. Environ. Sci. Technol. 15, 362–364. https://doi.org/10.1021/es00085a606

Meehan, W.J., Ostrander, G.K., 1997. Coral bleaching: A potential biomarker of environmental stress. J. Toxicol. Environ. Health 50, 529–552. https://doi.org/10.1080/15287399709532053

Metian, M., Hédouin, L., Ferrier-Pagès, C., Teyssié, J.L., Oberhansli, F., Buschiazzo, E., Warnau, M., 2015. Metal bioconcentration in the scleractinian coral Stylophora pistillata: investigating the role of different components of the holobiont using radiotracers. Environ. Monit. Assess. 187. https://doi.org/10.1007/s10661-015-4383-z

Millaleo, R., Reyes- Diaz, M., Ivanov, A.G., Mora, M.L., Alberdi, M., 2010. MANGANESE AS ESSENTIAL AND TOXIC ELEMENT FOR PLANTS: TRANSPORT, ACCUMULATION AND RESISTANCE MECHANISMS. J. Soil Sci. Plant Nutr. 10, 470–481. https://doi.org/10.4067/S0718-95162010000200008

Mitchelmore, C.L., Verde, E.A., Weis, V.M., 2007. Uptake and partitioning of copper and cadmium in the coral Pocillopora damicornis. Aquat. Toxicol. 85, 48–56. https://doi.org/10.1016/j.aquatox.2007.07.015

Morel, F.M.M., Price, N.M., 2003. The Biogeochemical Cycles of Trace Metals in the Oceans. Science 300, 944–947. https://doi.org/10.1126/science.1083545

Muscatine, L., 1990. The role of symbiotic algae in carbon and energy flux in reef corals. Ecosyst. World 25, 75–87.

Muscatine, L., Falkowski, P.G., Porter, J.W., Dubinsky, Z., 1984. Fate of Photosynthetic Fixed Carbon in Light- and Shade-Adapted Colonies of the Symbiotic Coral Stylophora pistillata. Proc. R. Soc. Lond. B Biol. Sci. 222, 181–202.

Oakes, K.D., Van Der Kraak, G.J., 2003. Utility of the TBARS assay in detecting oxidative stress in white sucker (Catostomus commersoni) populations exposed to pulp mill effluent. Aquat. Toxicol. 63, 447–463. https://doi.org/10.1016/S0166-445X(02)00204-7

Olgun, N., Duggen, S., Croot, P.L., Delmelle, P., Dietze, H., Schacht, U., Óskarsson, N., Siebe, C., Auer, A., Garbe-Schönberg, D., 2011. Surface ocean iron fertilization: The role of airborne volcanic ash from subduction zone and hot spot volcanoes and related iron fluxes into the Pacific Ocean. Glob. Biogeochem. Cycles 25. https://doi.org/10.1029/2009GB003761

Ono, S., Reimer, J.D., Tsukahara, J., 2002. Seasonal Changes in Zoanthus spp. in the Infra-Littoral Zone at Taisho Lava Field, Sakurajima, Kagoshima, Japan 22.

Oskarsson, N., 1980. The interaction between volcanic gases and tephra: Fluorine adhering to tephra of the 1970 hekla eruption. J. Volcanol. Geotherm. Res. 8, 251–266. https://doi.org/10.1016/0377-0273(80)90107-9

Pearson, C.L., Dale, D.S., Brewer, P.W., Kuniholm, P.I., Lipton, J., Manning, S.W., 2009. Dendrochemical analysis of a tree-ring growth anomaly associated with the Late Bronze Age eruption of Thera. J. Archaeol. Sci. 36, 1206–1214. https://doi.org/10.1016/j.jas.2009.01.009

Peters, E.C., Gassman, N.J., Firman, J.C., Richmond, R.H., Power, E.A., 1997. Ecotoxicology of tropical marine ecosystems. Environ. Toxicol. Chem. 16, 12–40. https://doi.org/10.1002/etc.5620160103

Ralph, P.J., Gademann, R., 2005. Rapid light curves: A powerful tool to assess photosynthetic activity. Aquat. Bot. 82, 222–237. https://doi.org/10.1016/j.aquabot.2005.02.006

Ralph, P.J., Larkum, A.W.D., Kühl, M., 2005. Temporal patterns in effective quantum yield of individual zooxanthellae expelled during bleaching. J. Exp. Mar. Biol. Ecol. 316, 17–28. https://doi.org/10.1016/j.jembe.2004.10.003

Ranjbar Jafarabadi, A., Riyahi Bakhtiari, A., Maisano, M., Pereira, P., Cappello, T., 2018. First record of bioaccumulation and bioconcentration of metals in Scleractinian corals and their algal symbionts from Kharg and Lark coral reefs (Persian Gulf, Iran). Sci. Total Environ. 640–641, 1500–1511. https://doi.org/10.1016/j.scitotenv.2018.06.029

Raven, J.A., Evans, M.C.W., Korb, R.E., 1999. The role of trace metals in photosynthetic electron transport in O2-evolving organisms. Photosynth. Res. 60, 111–150. https://doi.org/10.1023/A:1006282714942

Reguero, B.G., Beck, M.W., Agostini, V.N., Kramer, P., Hancock, B., 2018. Coral reefs for coastal protection: A new methodological approach and engineering case study in Grenada. J. Environ. Manage. 210, 146–161. https://doi.org/10.1016/j.jenvman.2018.01.024

Reich, H.G., Camp, E.F., Roger, L.M., Putnam, H.M., 2023. The trace metal economy of the coral holobiont: supplies, demands and exchanges. Biol. Rev. 98, 623–642. https://doi.org/10.1111/brv.12922

Reich, H.G., Rodriguez, I.B., LaJeunesse, T.C., Ho, T.Y., 2020. Endosymbiotic dinoflagellates pump iron: differences in iron and other trace metal needs among the Symbiodiniaceae. Coral Reefs 39, 915–927. https://doi.org/10.1007/s00338-020-01911-z

Reichelt-Brushett, A.J., Harrison, P.L., 1999. The Effect of Copper, Zinc and Cadmium on Fertilization Success of Gametes from Scleractinian Reef Corals. Mar. Pollut. Bull. 38.

Reichelt-Brushett, A.J., McOrist, G., 2003. Trace metals in the living and nonliving components of scleractinian corals. Mar. Pollut. Bull. 46, 1573–1582. https://doi.org/10.1016/S0025-326X(03)00323-0

Reynaud, S., Ferrier-Pagès, C., Sambrotto, R., Juillet-Leclerc, A., Jaubert, J., Gattuso, J.-P., 2002. Effect of feeding on the carbon and oxygen isotopic composition in the tissues and skeleton of the zooxanthellate coral Stylophora pistillata. Mar. Ecol. Prog. Ser. Mar Ecol Prog Ser 238, 81–89.

Rijstenbil, J.W., Derksen, J.W.M., Gerringa, L.J.A., Poortvliet, T.C.W., Sandee, A., van den Berg, M., van Drie, J., Wijnholds, J.A., 1994. Oxidative stress induced by copper: defense and damage in the marine planktonic diatom Ditylum brightwellii, grown in continuous cultures with high and low zinc levels. Mar. Biol. 119, 583–590. https://doi.org/10.1007/BF00354321

Ritchie, R.J., 2006. Consistent Sets of Spectrophotometric Chlorophyll Equations for Acetone, Methanol and Ethanol Solvents. Photosynth. Res. 89, 27–41. https://doi.org/10.1007/s11120-006-9065-9

Rodriguez, I.B., Lin, S., Ho, J., Ho, T.Y., 2016. Effects of trace metal concentrations on the growth of the coral endosymbiont Symbiodinium kawagutii. Front. Microbiol. 7. https://doi.org/10.3389/fmicb.2016.00082

Sabdono, A., 2009. Heavy metal levels and their potential toxic effect on coral Galaxea fascicularis from Java Sea, Indonesia. Res. J. Environ. Sci. 3, 96–102.

Savage, C., 2019. Seabird nutrients are assimilated by corals and enhance coral growth rates. Sci. Rep. 9, 4284. https://doi.org/10.1038/s41598-019-41030-6

Schils, T., 2012. Episodic Eruptions of Volcanic Ash Trigger a Reversible Cascade of Nuisance Species Outbreaks in Pristine Coral Habitats. PLoS ONE 7. https://doi.org/10.1371/journal.pone.0046639

Seefeldt, L.C., Hoffman, B.M., Dean, D.R., 2009. Mechanism of Mo-Dependent Nitrogenase. Annu. Rev. Biochem. 78, 701–722. https://doi.org/10.1146/annurev.biochem.78.070907.103812

Self, S., 2006. The effects and consequences of very large explosive volcanic eruptions. Philos. Trans. R. Soc. Math. Phys. Eng. Sci. 364, 2073–2097. https://doi.org/10.1098/rsta.2006.1814

Shaw, B.P., Sahu, S.K., Mishra, R.K., 2004. Heavy Metal Induced Oxidative Damage in Terrestrial Plants, in: Prasad, M.N.V. (Ed.), Heavy Metal Stress in Plants: From Biomolecules to Ecosystems. Springer Berlin Heidelberg, Berlin, Heidelberg, pp. 84–126. https://doi.org/10.1007/978-3-662-07743-6_4

Siebert, L., Cottrell, E., Venzke, E., Andrews, B., 2015. Earth's Volcanoes and Their Eruptions: An Overview, in: The Encyclopedia of Volcanoes. Elsevier, pp. 239–255. https://doi.org/10.1016/B978-0-12-385938-9.00012-2

Smallhorn-West, P.F., Garvin, J.B., Slayback, D.A., DeCarlo, T.M., Gordon, S.E., Fitzgerald, S.H., Halafihi, T., Jones, G.P., Bridge, T.C.L., 2020. Coral reef annihilation, persistence and recovery at Earth's youngest volcanic island. Coral Reefs 39, 529–536. https://doi.org/10.1007/s00338-019-01868-8

Smith, P.K., Krohn, R.I., Hermanson, G.T., Mallia, A.K., Gartner, F.H., Provenzano, M.D., Fujimoto, E.K., Goeke, N.M., Olson, B.J., Klenk, D.C., 1985. Measurement of protein using bicinchoninic acid. Anal. Biochem. 150, 76–85. https://doi.org/10.1016/0003-2697(85)90442-7

Souter, D., Planes, S., Wicquart, J., Obura, D., Staub, F., 2021. Status of Coral Reefs of the World: 2020. International Coral Reef Initiative. https://doi.org/10.59387/WOTJ9184

Sparks, R.S.J., Bursik, M.I., Ablay, G.J., Thomas, R.M.E., Carey, S.N., 1992. Sedimentation of tephra by volcanic plumes. Part 2: controls on thickness and grain-size variations of tephra fall deposits. Bull. Volcanol. 54, 685–695. https://doi.org/10.1007/BF00430779

Stewart, C., Damby, D.E., Tomašek, I., Horwell, C.J., Plumlee, G.S., Armienta, M.A., Hinojosa, M.G.R., Appleby, M., Delmelle, P., Cronin, S., Ottley, C.J., Oppenheimer, C., Morman, S., 2020. Assessment of leachable elements in volcanic ashfall: a review and evaluation of a standardized protocol for ash hazard characterization. J. Volcanol. Geotherm. Res. 392. https://doi.org/10.1016/j.jvolgeores.2019.106756

Stewart, C., Johnston, D.M., Leonard, G.S., Horwell, C.J., Thordarson, T., Cronin, S.J., 2006. Contamination of water supplies by volcanic ashfall: A literature review and simple impact modelling. J. Volcanol. Geotherm. Res. 158, 296–306. https://doi.org/10.1016/j.jvolgeores.2006.07.002

Stimson, J., Kinzie, R.A., 1991. The temporal pattern and rate of release of zooxanthellae from the reef coral Pocillopora damicornis (Linnaeus) under nitrogen-enrichment and control conditions. J. Exp. Mar. Biol. Ecol. 63–74.

Tambutté, S., Holcomb, M., Ferrier-Pagès, C., Reynaud, S., Tambutté, É., Zoccola, D., Allemand, D., 2011. Coral biomineralization: from the gene to the environment. J. Exp. Mar. Biol. Ecol. 408, 58–78. https://doi.org/10.1016/j.jembe.2011.07.026

Twining, B.S., Baines, S.B., 2013. The Trace Metal Composition of Marine Phytoplankton. Annu. Rev. Mar. Sci. 5, 191–215. https://doi.org/10.1146/annurev-marine-121211-172322

Uematsu, M., Toratani, M., Kajino, M., Narita, Y., Senga, Y., Kimoto, T., 2004. Enhancement of primary productivity in the western North Pacific caused by the eruption of the Miyake-jima Volcano: ENHANCED PRODUCTION BY VOLCANIC ERUPTION. Geophys. Res. Lett. 31, n/a-n/a. https://doi.org/10.1029/2003GL018790

Van Wert, J.C., Ezzat, L., Munsterman, K.S., Landfield, K., Schiettekatte, N.M.D., Parravicini, V., Casey, J.M., Brandl, S.J., Burkepile, D.E., Eliason, E.J., 2023. Fish feces reveal diverse nutrient sources for coral reefs. Ecology 104, e4119. https://doi.org/10.1002/ecy.4119

Van Zanten, B.T., Van Beukering, P.J.H., Wagtendonk, A.J., 2014. Coastal protection by coral reefs: A framework for spatial assessment and economic valuation. Ocean Coast. Manag. 96, 94–103. https://doi.org/10.1016/j.ocecoaman.2014.05.001

Vroom, P.S., Zgliczynski, B.J., 2011. Effects of volcanic ash deposits on four functional groups of a coral reef. Coral Reefs 30, 1025–1032. https://doi.org/10.1007/s00338-011-0793-8

Wall-Palmer, D., Jones, M.T., Hart, M.B., Fisher, J.K., Smart, C.W., Hembury, D.J., Palmer, M.R., Fones, G.R., 2011. Explosive volcanism as a cause for mass mortality of pteropods. Mar. Geol. 282, 231–239. https://doi.org/10.1016/j.margeo.2011.03.001

Witham, C.S., Oppenheimer, C., Horwell, C.J., 2005. Volcanic ash-leachates: A review and recommendations for sampling methods. J. Volcanol. Geotherm. Res. 141, 299–326. https://doi.org/10.1016/j.jvolgeores.2004.11.010

Wu, C.C., Shen, C.C., Lo, L., Hsin, Y.C., Yu, K., Chang, C.C., Lam, D.D., Chou, Y.M., Liu, Y., Pallister, J., Song, S.R., Chiang, H.W., Burr, G.S., 2018. Pinatubo Volcanic Eruption Exacerbated an Abrupt Coral Mortality Event in 1991 Summer. Geophys. Res. Lett. 45, 12,396-12,402. https://doi.org/10.1029/2018GL079529

Wygel, C.M., Peters, S.C., McDermott, J.M., Sahagian, D.L., 2019. Bubbles and Dust: Experimental Results of Dissolution Rates of Metal Salts and Glasses From Volcanic Ash Deposits in Terms of Surface Area, Chemistry, and Human Health Impacts. GeoHealth 3, 338–355. https://doi.org/10.1029/2018GH000181

Xu, Y., Zhang, Jing, Huang, H., Yuan, X., Zhang, Junxiao, Ge, J., 2022. Coral Symbiosis Carbon Flow: A Numerical Model Study Spanning Cellular to Ecosystem Levels. Front. Mar. Sci. 9.

Author Contributions Statement

All authors contributed meaningfully to this work. Frank Förster is the primary author and contributed to all aspects of the manuscript. Stéphanie Reynaud contributed to supervision, sample preparation, idea conceptualization, initial results analysis and editing. Lucie Sauzéat contributed to data collection, writing, results analysis, and editing. Christine Ferrier-Pagès contributed to supervision, idea conceptualization, initial results analysis and editing. Elias Samankassou contributed to establishing the connection to the Centre Scientifique de Monaco, and editing. Tom Sheldrake contributed to supervision, idea conceptualization, results analysis and editing.

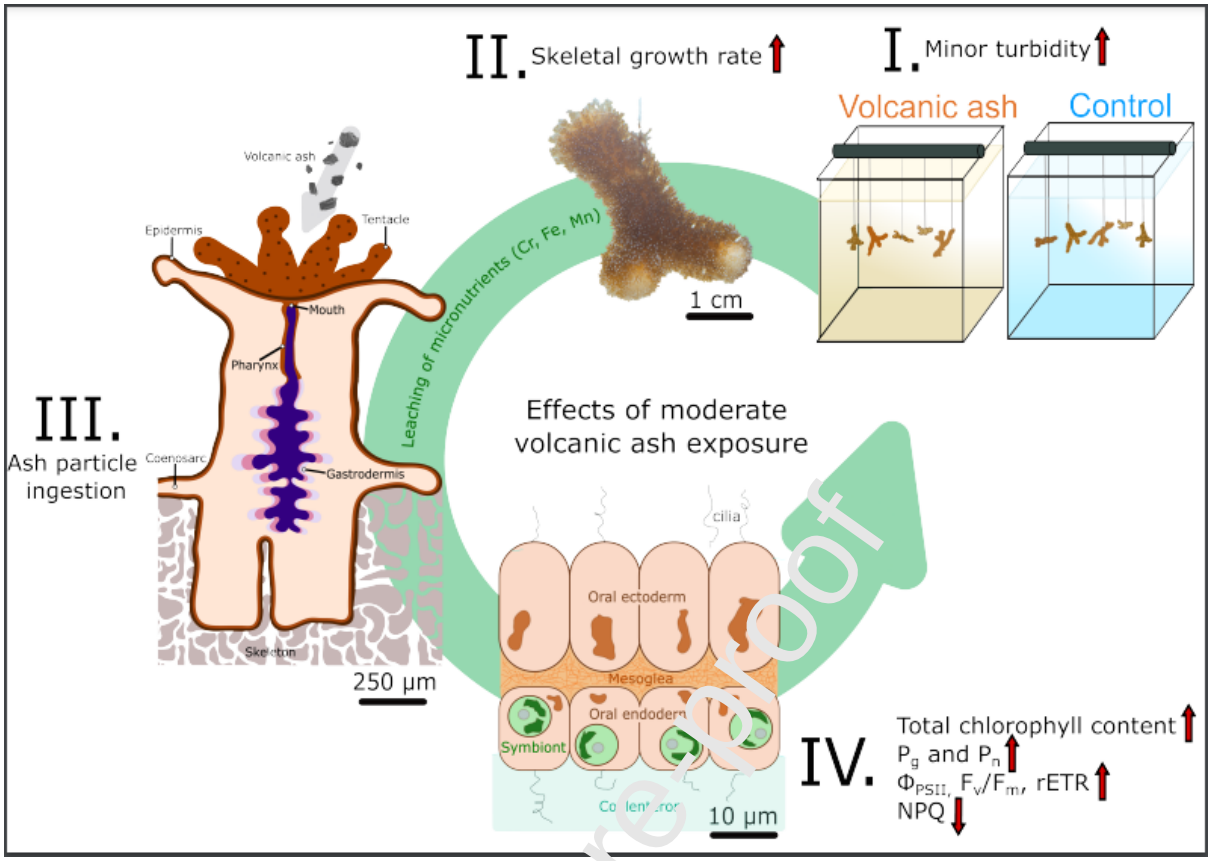

Highlights

- First laboratory assessment of the interaction between volcanic ash and corals
- Leaching of volcanic ash supplies the coral with important micronutrients
- Rapid enhancement of the photosynthetic performance of Symbiodiniaceae
- Increased biomineralization rates after weeks of constant ash supply

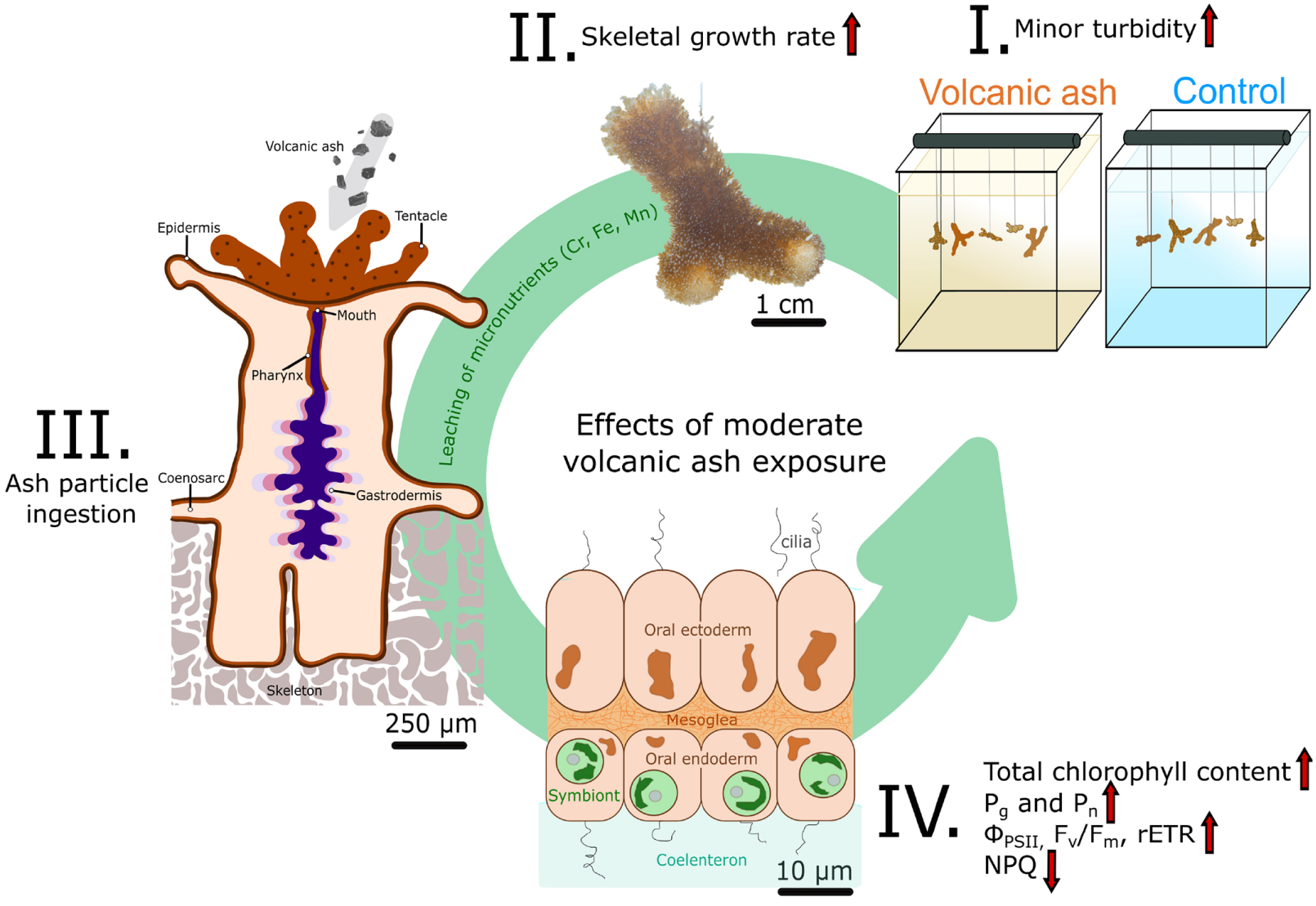

Graphics Abstract

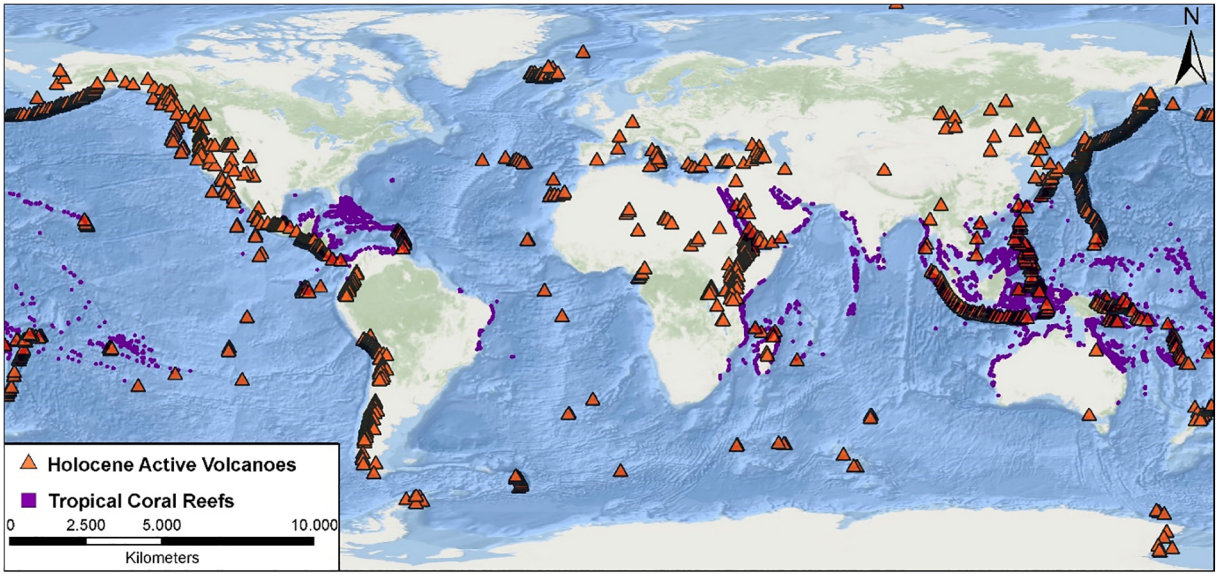
N
Holocene Active Volcanoes
Tropical Coral Reefs
0
2.500
5.000
10.000
Kilometers

Figure 1

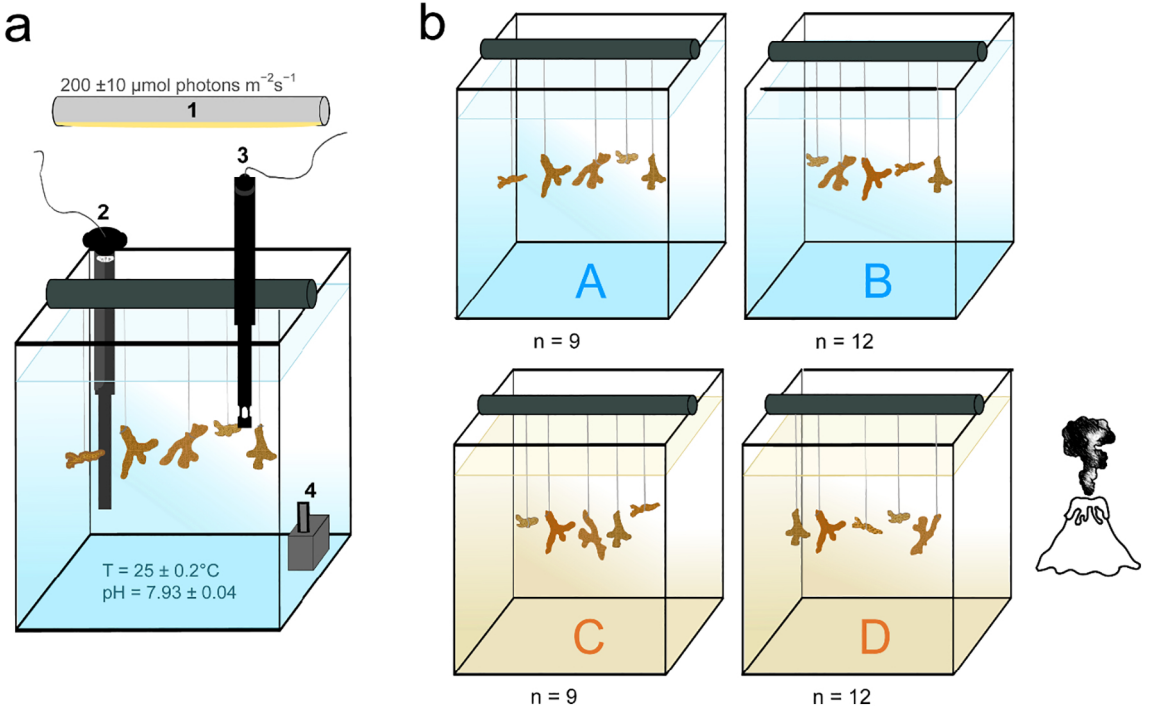
a
200 ±10 µmol photons m^{-2}s^{-1}
1
2
3
4
T = 25 ± 0.2°C
pH = 7.93 ± 0.04
b
A
B
n = 9
n = 12
C
D
n = 9
n = 12

Figure 2

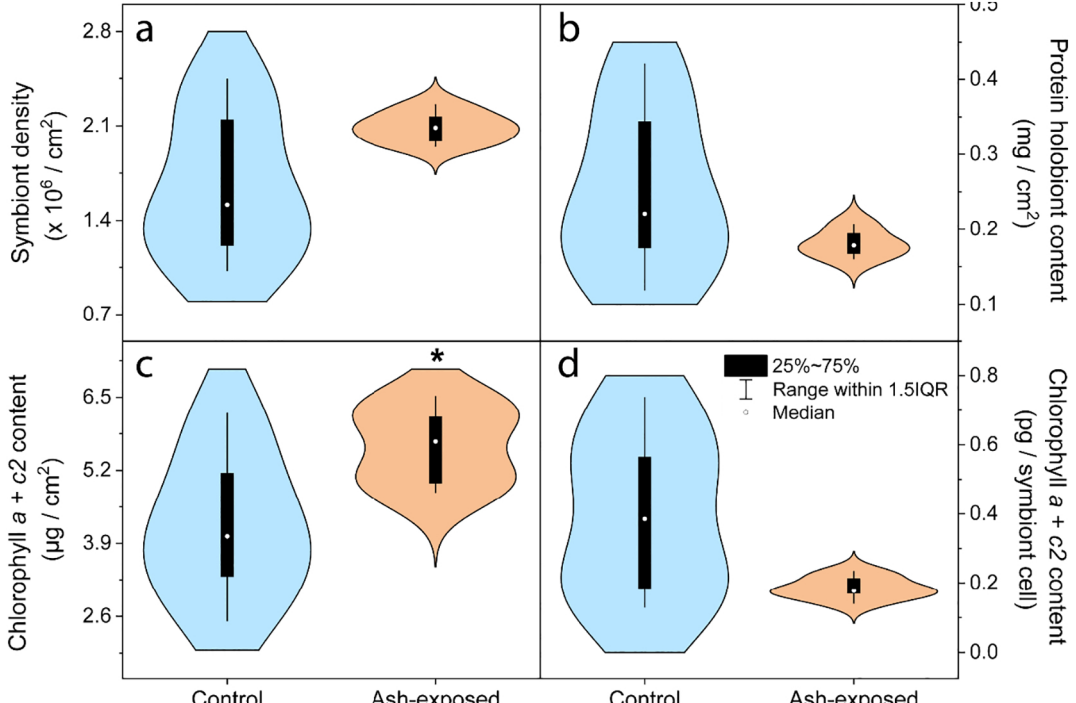
a
b
c
d
Symbiont density (x 10^6 / cm^2)
Protein holobiont content (mg / cm^2)
Chlorophyll a + c2 content (µg / cm^2)
Chlorophyll a + c2 content (pg / symbiont cell)
2.8
2.1
1.4
0.7
0.5
0.4
0.3
0.2
0.1
6.5
5.2
3.9
2.6
0.8
0.6
0.4
0.2
0.0
*
25%~75%
Range within 1.5IQR
Median
Control
Ash-exposed
Control
Ash-exposed

Figure 3

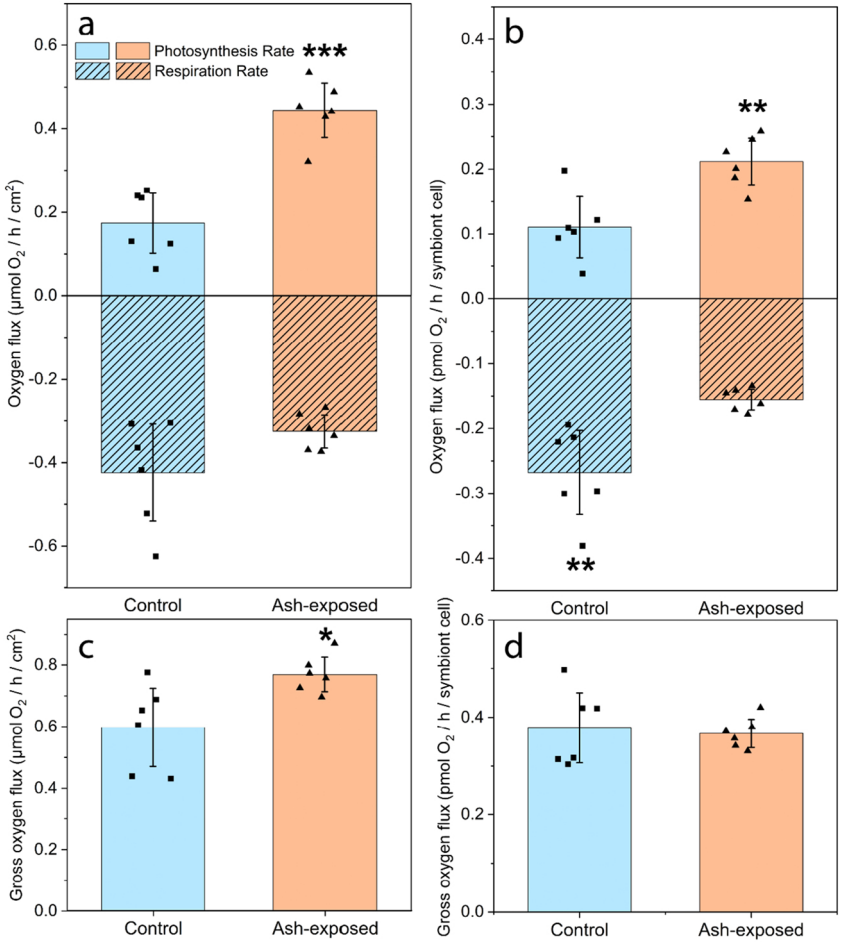
a
Photosynthesis Rate
Respiration Rate
***
Oxygen flux (μmol O2 / h / cm2)
0.6
0.4
0.2
0.0
-0.2
-0.4
-0.6
Control
Ash-exposed
b
**
**
Oxygen flux (pmol O2 / h / symbiont cell)
0.4
0.3
0.2
0.1
0.0
-0.1
-0.2
-0.3
-0.4
Control
Ash-exposed
c
*
Gross oxygen flux (μmol O2 / h / cm2)
0.8
0.6
0.4
0.2
0.0
Control
Ash-exposed
d
Gross oxygen flux (pmol O2 / h / symbiont cell)
0.6
0.4
0.2
0.0
Control
Ash-exposed

Figure 4

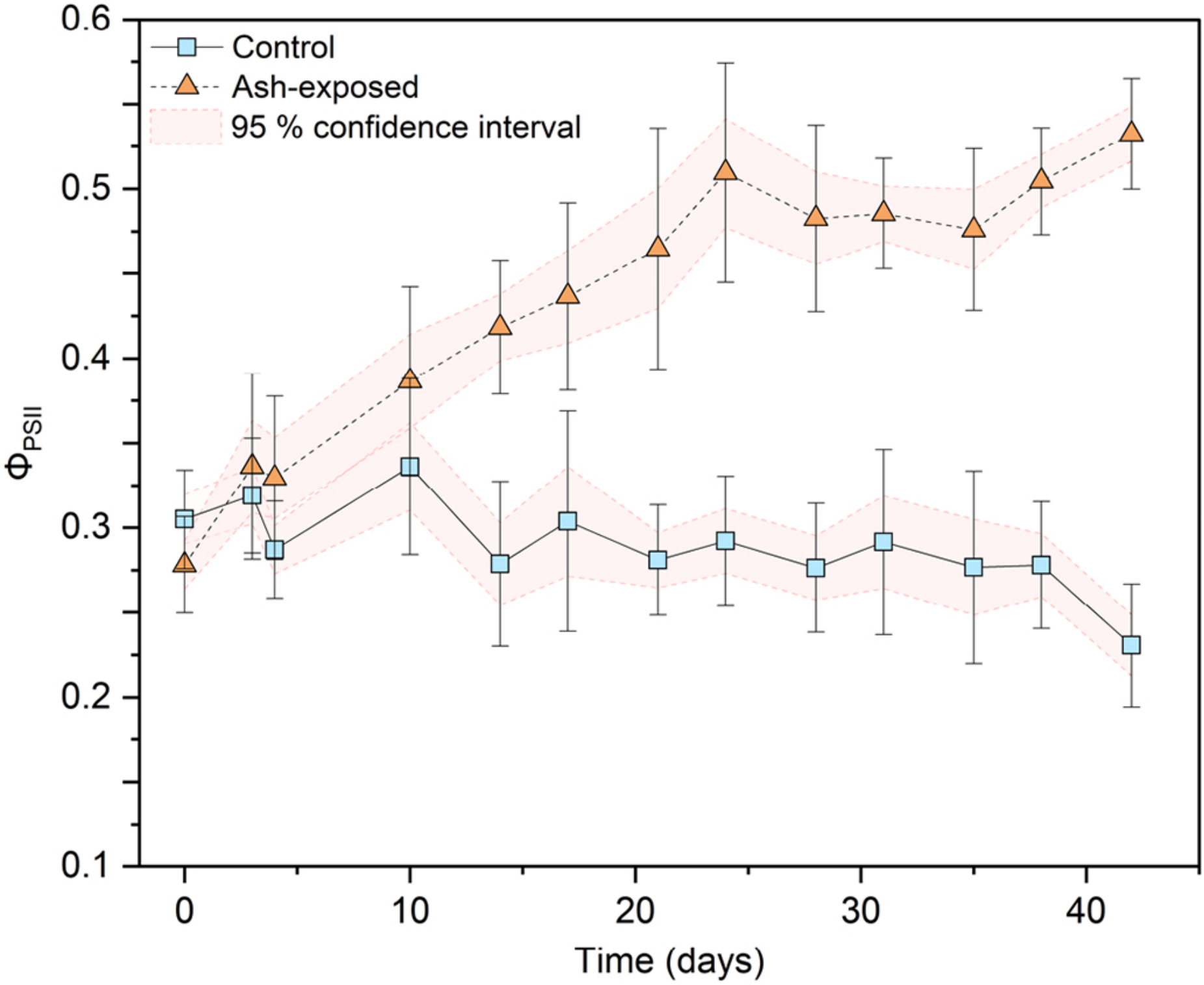
Control
Ash-exposed
95 % confidence interval
Φ_{PSII}
0.6
0.5
0.4
0.3
0.2
0.1
0
10
20
30
40
Time (days)

Figure 5

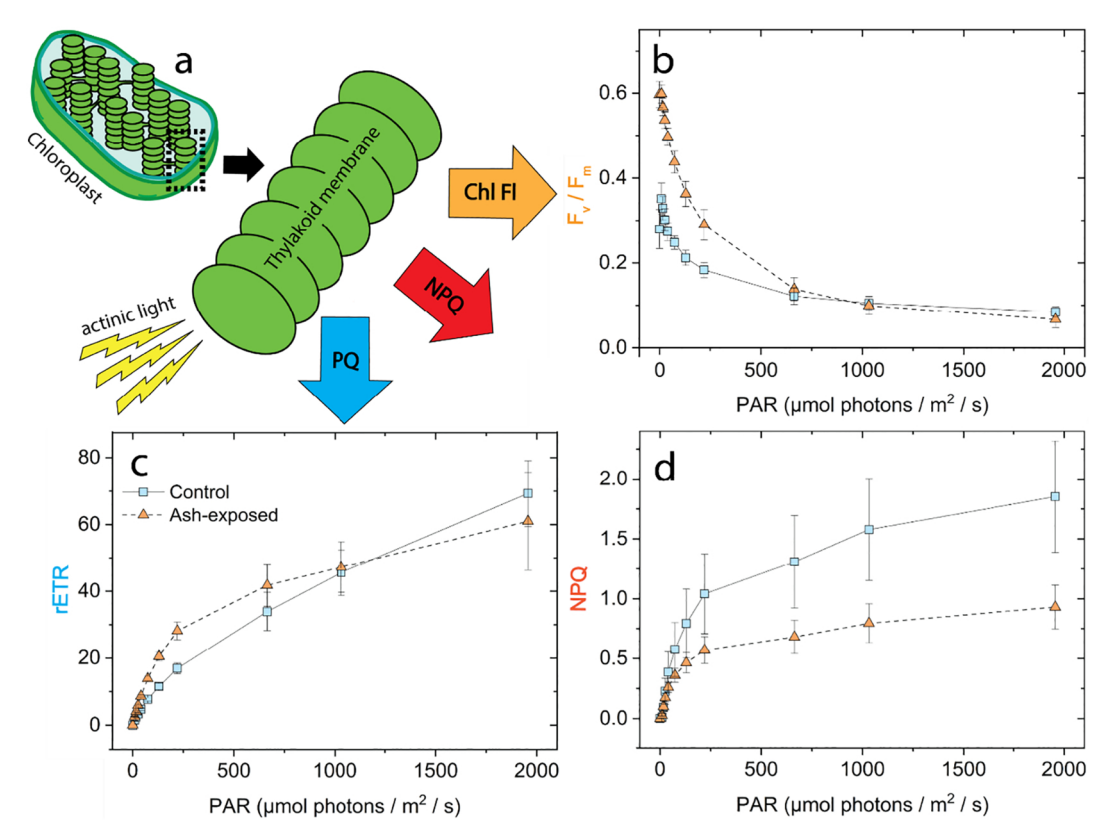
a
Chloroplast
Thylakoid membrane
Chl Fl
NPQ
PQ
actinic light
b
F_v / F_m
PAR (µmol photons / m² / s)
c
Control
Ash-exposed
rETR
PAR (µmol photons / m² / s)
d
NPQ
PAR (µmol photons / m² / s)

Figure 6

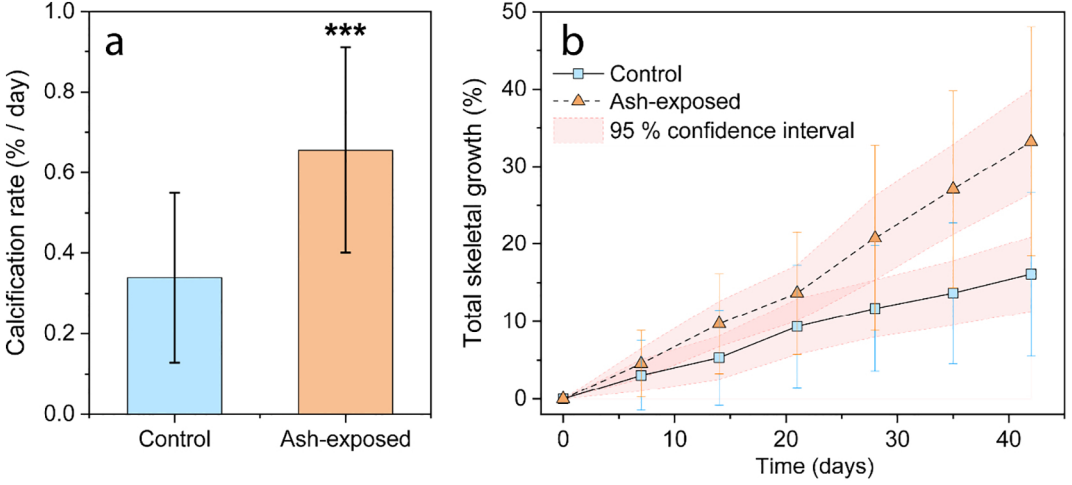
a
***
Calcification rate (% / day)
1.0
0.8
0.6
0.4
0.2
0.0
Control
Ash-exposed
b
Control
Ash-exposed
95 % confidence interval
Total skeletal growth (%)
50
40
30
20
10
0
0
10
20
30
40
Time (days)

Figure 7

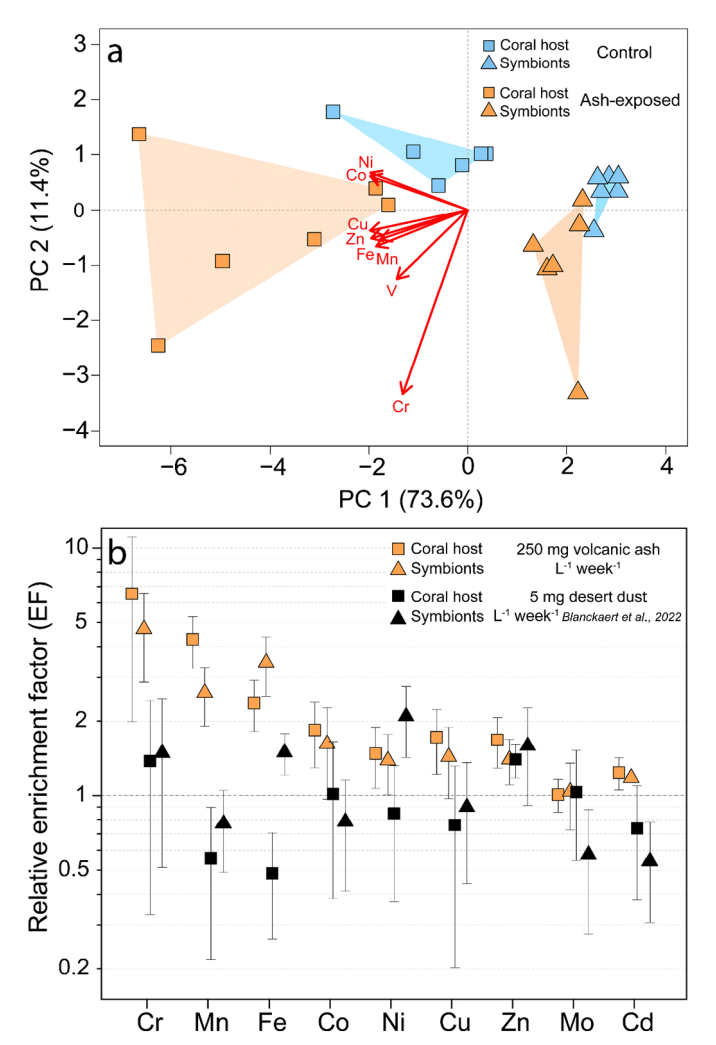
a
Coral host
Symbionts
Control
Coral host
Symbionts
Ash-exposed
Ni
Co
Cu
Zn
Fe
Mn
V
Cr
PC 2 (11.4%)
PC 1 (73.6%)
b
Coral host
Symbionts
250 mg volcanic ash L-1 week-1
Coral host
Symbionts
5 mg desert dust L-1 week-1 Blanckaert et al., 2022
Relative enrichment factor (EF)
Cr
Mn
Fe
Co
Ni
Cu
Zn
Mo
Cd

Figure 8